NASA CONTRACTOR REPORT

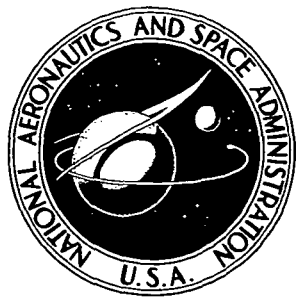

NASA CR-2494

NASA CR-2494

SIMULATION OF HYPERSONIC SCRAMJET EXHAUST

R. A. Oman, K. M. Foreman, J. Leng, and H. B. Hopkins

Prepared by
GRUMMAN AEROSPACE CORPORATION
Bethpage, N.Y. 11714
for Langley Research Center

NATIONAL AERONAUTICS AND SPACE ADMINISTRATION • WASHINGTON, D. C. • MARCH 1975

1. Report No.	2. Government Accession No.	3. Recipient's Catalog No.
NASA CR-2494		

4. Title and Subtitle	5. Report Date
SIMULATION OF HYPERSONIC SCRAMJET EXHAUST	MARCH 1975
	6. Performing Organization Code
7. Author(s)	8. Performing Organization Report No.
R. A. Oman, K. M. Foreman, J. Leng, and H. B. Hopkins	RE-473
	10. Work Unit No.
9. Performing Organization Name and Address	760-66-01-02-00
Grumman Aerospace Corporation Bethpage, N.Y. 11714	11. Contract or Grant No.
	NAS1-12553
	13. Type of Report and Period Covered
12. Sponsoring Agency Name and Address	CONTRACTOR REPORT
National Aeronautics and Space Administration Washington, D.C. 20546	14. Sponsoring Agency Code

15. Supplementary Notes

FINAL REPORT

16. Abstract

This report describes a plan and some preliminary analysis for the accurate simulation of pressure distributions on the afterbody/nozzle portions of a hypersonic scramjet vehicle. The objectives fulfilled were to establish the standards of similitude for a hydrogen/air scramjet exhaust interacting with a vehicle afterbody, determine an experimental technique for validation of the procedures that will be used in conventional wind tunnel facilities, suggest a program of experiments for proof of the concept, and explore any unresolved problems in the proposed simulation procedures. It is shown that true enthalpy, Reynolds number, and nearly exact chemistry can be provided in the exhaust flow for the flight regime from Mach 4 to 10 by a detonation tube simulation. A detailed discussion of the required similarity parameters leads to the conclusion that substitute gases can be used as the simulated exhaust gas in a wind tunnel to achieve the correct interaction forces and moments. A proof-of-concept series of experiments is proposed using the detonation tube as a standard against which substitute gas candidates would be compared. Detailed procedures for selecting the binary mixtures for substitute gas blends are presented, along with calculated comparisons of pressures and forces for the real engine case, the detonation tube case, and two representative substitute gas mixtures.

17. Key Words (Suggested by Author(s))	18. Distribution Statement
Engine/Airframe Integration Hypersonic Simulation Scramjet	Unclassified - Unlimited Subject category 05 Aircraft Design, Testing and Performance

19. Security Classif. (of this report)	20. Security Classif. (of this page)	21. No. of Pages	22. Price*
Unclassified	Unclassified	71	$4.25

*For sale by the National Technical Information Service, Springfield, Virginia 22151

TABLE OF CONTENTS

SIMULATION OF HYPERSONIC SCRAMJET EXHAUST

By R. A. Oman, K. M. Foreman, J. Leng, and H. B. Hopkins
Research Department
Grumman Aerospace Corporation
Bethpage, New York 11714

INTRODUCTION AND SUMMARY

This report describes a plan and some preliminary analysis for the accurate simulation of pressure distributions on the afterbody/nozzle portions of a hypersonic scramjet vehicle such as shown in the figure on page 2. It is apparent from the current design philosophy for these vehicles that the scramjet exhaust gases will play a major role in the determination of the aerodynamic forces and moments acting on the vehicle. Conventional aerodynamic testing methods offer no straightforward approach that will meet all of the vehicle development requirements. In this first investigation our objectives were to establish the standards of similitude for a hydrogen/air scramjet exhaust interacting with a vehicle afterbody, determine an experimental technique for validation of the procedures that will be used in conventional wind tunnel facilities, suggest a program of experiments for proof of the concept, and explore any unresolved problems in the proposed simulation procedures. We have fulfilled all of these objectives, and the second phase activities of proof-of-concept experiments and more detailed analysis are ready to begin.

The over-all plan for vehicle development that we have defined during the program covered by this report has four separate activities that culminate in a final determination of the afterbody pressure distribution in a wind tunnel. First, the expansion characteristics of the hydrogen/air combustion products at true flight enthalpy will be determined by pressure and other diagnostic measurements in a special facility called a detonation tube simulator. Second, a small number of substitute gases will be tested in the same facility to show that they are capable of reproducing at moderate temperature levels the pressure distributions of the hot combustion products. Third, a series of experiments will be conducted with substitute gases and with combustion products to develop methods for assessing such nonuniformities as

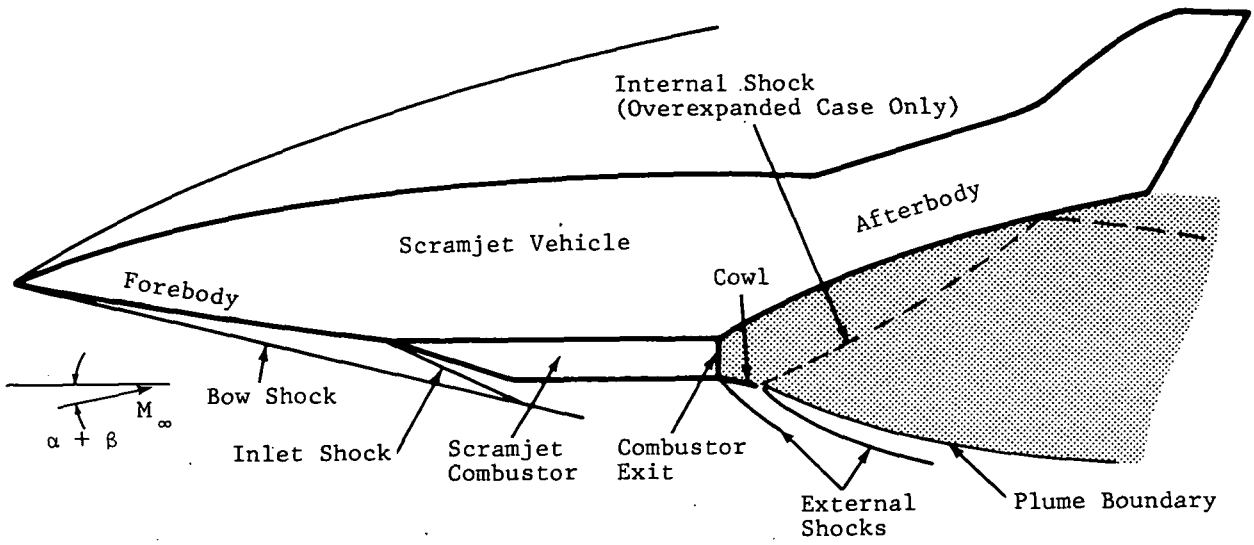

Side View

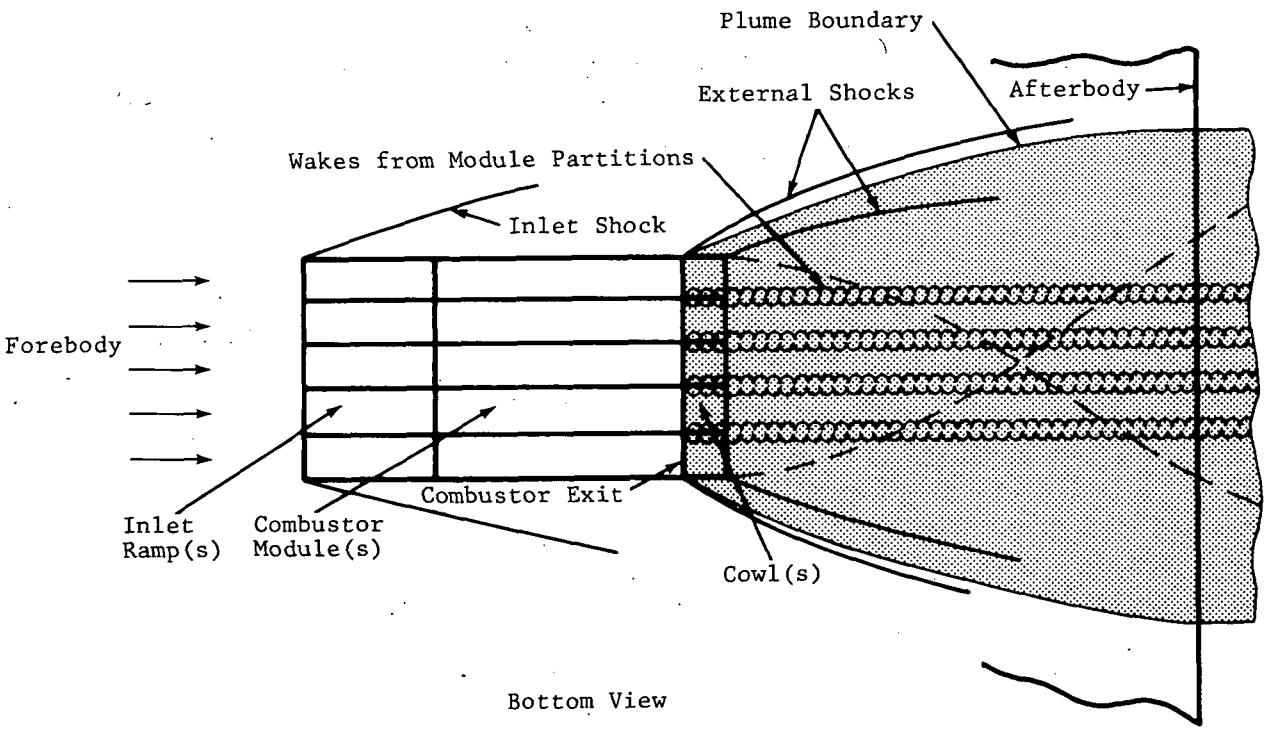

Bottom View

Scramjet Nozzle and Related Flow Fields

combustor partition wakes, combustor wall boundary layers, corner flows, and combustor end effects. Fourth, the qualified substitute gases will be used in vehicle and combustor development testing in conventional wind tunnel facilities. The four activities can, in part, run concurrently.

One of the most difficult simulation problems for the scramjet exhaust is to reproduce the effect of the correct chemistry along with the high total enthalpy (flight compression plus combustion heating) in the exhaust flow. To achieve this combination with the true combustion mixture in a conventional wind tunnel model of reasonable size and complexity is a virtual impossibility. The approach we have taken in the current work is to investigate the use of a cold substitute gas, or blend of gases, to simulate the scramjet exhaust. In order to select such a substitute gas, we must have a comparison technique for validating the gas mixtures chosen to represent the exhaust at different flight conditions. The best validation will come from measurement of actual pressure distributions over a scale model of the vehicle afterbody with an exhaust gas consisting of the products of combustion of hydrogen and air at an enthalpy level as close to that of the real engine as possible. These pressure distributions can then be compared to those obtained with selected substitute gas mixtures.

An extensive analysis of the requirements that must be fulfilled to ensure fidelity of model pressure distributions to the flight case showed that the most critical parameters were matching combustor exit Mach number and following the variation of specific heat ratio with increasing M in an isentropic expansion. Many other important simulation requirements have also been satisfied by the plan we have devised. The requirements of pressure simulation within the diverging contact surfaces of the underexpanded exhaust are met to a remarkable degree. Reynolds number is matched, Prandtl number is quite closely matched, and the viscosity variation through the boundary layer is shown to be nearly that needed for an ideal boundary layer match. Slight adjustments in the substitute gas blends can easily be made to allow for different degrees of chemical equilibrium in the flight exhaust. Even the strict similitude requirements of the turbulent mixing layer between exhaust and external flow could be fulfilled by the substitute gases if they were used in a special Freon wind tunnel — but we recommend a separate investigation of hypersonic mixing layer similitude for the purpose of easing this requirement. In short, the substitute gas

concept looks like a valid approach, and the next step is to prove it by comparison to a valid standard flow.

The only known technique for producing the correct enthalpy and chemistry in the laboratory appears to be the detonation tube concept pioneered by Grumman for the LM program, and used subsequently to simulate the exhaust from the hydrogen/oxygen main engines for the Space Shuttle (Ref. 1). This technique is ideally suited to scramjet simulation because it combines shock heating of the gas with the heat of combustion to obtain the required enthalpy. One of the main objectives of our current work was to investigate analytically the operating range of the detonation tube facility and to match it to the proposed flight envelope of the scramjet aircraft. We have done this and shown the technique to be capable of high quality simulation throughout the complete flight regime and beyond. Having shown that operating range is not a significant problem for the detonation tube system, we selected a nominal Mach 8 flight condition as a baseline condition for the first set of demonstration tests. Picking a single flight Mach number restricts the required model building to a set with one exit area ratio yet allows a full range of experiments on pressure and enthalpy levels, substitute gas matching, and exit plane partition wakes.

The next objective was to examine and select possible substitute gases for subsequent experiments. Three promising binary mixtures were chosen, and two dimensional pressure distributions were calculated for the flight baseline conditions on the real engine, the detonation tube simulation, and the three substitute gases. The selection procedures involved a one dimensional screening technique, after which the two dimensional method of characteristics calculations were made to compare actual pressure distributions over the two dimensional representation of the geometry that we propose to test in the next phase. On page 5, we show a preview of Fig. 16, which describes better than words the matches of axial and normal forces that we can get. The blends used are easily prepared and modified, safe, and relatively inexpensive. Although only inviscid flows are shown, the friction drag will also be properly scaled when normalized by the exit plane pressure.

In summary, the results of the present investigation show that the detonation tube simulator should provide an excellent simulation of the hydrogen/air scramjet exhaust flow over the vehicle afterbody for the entire flight regime. There are

several nontoxic, relatively inexpensive substitute gas mixtures available for use in wind tunnels that will give adequate represenations of the pressure distributions over the afterbody due to the scramjet exhaust. In order to choose the best substitute gas mixture for a given flight regime, comparisons with the detonation tube results and with mixing layer similitude requirements will be made. An experimental program to prove this concept at a representative point in the flight envelope is presented. We expect that such a program will provide the ability to simulate correctly the aerodynamic loads due to the engine exhaust in subsequent experiments in Langley facilities.

Relative Normal Forces

$$\frac{Fy}{P_3A} = \frac{1}{L}\int \frac{P}{P_3}\, d(x)$$

Prototype - Equilibrium	0.0339	
Prototype - Frozen	0.0279	
Model - 1/8th Scale Det. Tube	0.0301	
Model - Sub. Gas	0.0339	50% Freon 13 B1, 50% Ar
Model - Sub. Gas	0.0292	40% Freon 12,60% Ar
Model - Sub. Gas	0.0344	58% Freon 13 B1 + 42% Ar
0.00351	Const. γ (=1.4)	

Relative Axial Forces

$$\frac{Fx}{P_3A} = \frac{1}{L}\int \frac{P}{P_3}\, d(y)$$

Prototype - Equilibrium	0.0648
Prototype - Frozen	0.0620
Model - 1/8th Scale Detonation Tube - Equilibrium	0.0634
Model - Sub. Gas - 50% Freon 13B1, 50% Ar	0.0646
Model - Sub. Gas - 40% Freon 12, 60% Ar	0.0627
Model - Sub. Gas - 58% Freon 13 B1 + 42% Ar	0.0647
Const.γ (=1.4)	0.0520

Normal and Axial Forces for 2D Expansions
$M_\infty = 8, \alpha + \beta = 4^\circ$

SYMBOLS

A	area
Ar	argon atom
a	sound speed
c_p	specific heat at constant pressure
c_v	specific heat at constant volume
D_{12}	binary diffusion coefficient, defined on page 64
D_I	first Damköhler parameter, defined on page 15
D_{III}	third Damköhler parameter, defined on page 16
Ec	Eckert number, defined on page 16
F	fluorine atom; also abreviation for Freon
Freon 12	dichlorodifluoromethane (CCl_2F_2)
Freon 13	chlorotrifluoromethane ($CClF_3$)
Freon 13B1	bromotrifluoromethane ($CBrF_3$)
Freon 14	tetrafluoromethane (CF_4)
Freon E5	a complex fluorinated ether
H	enthalpy; also hydrogen atom
HFA	hydrogen fueled aircraft
K	Kelvin temperature scale
k	thermal conductivity
L	length
LM	NASA/Grumman Lunar Module

Le	Lewis number, defined on page 15
M	Mach number ($\equiv V/a$)
$\mathcal{m}$	molecular weight
m	unit of length (meter)
N	nitrogen atom; also unit of force (Newton)
Nu	Nusselt number, defined on page 17
n	exponent in temperature-viscosity power law
O	oxygen atom
P	pressure
Pr	Prandtl number, defined on page 14
$\dot{q}$	heat transfer rate
R	universal gas constant
Re	Reynolds number ($\equiv \rho VL/\mu$)
S	sulphur atom; also entropy
SCRJ	Supersonic Combustion Ramjet
Sc	Schmidt number, defined on page 15
T	temperature
t	time
U	velocity (in detonation tube)
V	velocity
X	coefficient in chemical mixture equation (pp. 34 and 61); also afterbody axial distance
$\bar{X}$	nondimensional distance ($\equiv X/Y_3$)

Y	coefficient in chemical mixture equation, page 34; also afterbody radial distance
$\bar{Y}$	nondimensional distance ($\equiv Y/Y_3$)
α	angle of attack
β	inlet ramp angle
γ	ratio of specific heats, c_p/c_v
$\bar{\gamma}$	average γ between two frozen thermodynamic states
$\bar{\gamma}^c$	average γ between two equilibrium thermodynamic states
θ	temperature difference between two points
μ	viscosity, or prefix "micro" (10^{-6})
ρ	density
σ	thermodynamic function defined on page 34; also molecular collision diameter constant defined on page 64
τ	ratio of two different absolute temperatures
ϕ	equivalence ratio
φ	mixture viscosity parameter defined on page 62

Subscripts

o	refers to total (stagnation) condition
1	refers to an arbitrary thermodynamic state point
2	refers to an arbitrary thermodynamic state point; also thermodynamic state behind incident shock wave in detonation tube

3	refers to combustor exit plane
4	refers to unexpanded, high pressure driver gas
5	refers to stagnation condition or region behind reflected shock wave in detonation tube
∞	refers to undisturbed free stream
CJ	refers to Chapman-Jouguet thermodynamic state
i	refers to i^{th} chemical specie; also internal flow
e	refers to external flow; also shock tube nozzle exit plane
m	refers to a mixture of gases
s	refers to constant entropy

Superscript

*	refers to sonic condition

SIMILITUDE AND SUBSTITUTE GASES

The purpose of this part of the investigation is to identify the thermodynamic and transport property relationships necessary to ensure that the flow fields of scaled test nozzles will produce the same pressure distributions as those of the full scale exhaust nozzles used in supersonic combustion ramjets (SCRJ). Because of the method selected to achieve this result, a critical associated task is the selection of suitable test gases to be substituted in wind tunnel tests for the extremely high temperature exhaust gases produced by the hydrogen fueled aircraft (HFA).

The nondimensional similarity parameters for inviscid and viscous flow are computed for the SCRJ and used to formulate substitute gases with the required properties, assuming geometric similarity between the model and full scale nozzle configurations. A significant effort has been required to compile the most current and authoritative transport properties for the likely substitute gas constituents and to determine the most accurate combining rules for estimating transport properties of the gas mixtures. Sixteen gases considered safe, easily handled, chemically stable, relatively inexpensive, and commercially available were considered. The most promising substitute gas blends (binary mixtures) from those sixteen were determined by the following four-step matching process. Initially, for specific flight conditions, the combustor exit specific heat ratio, γ_3, and the approximate range of γ variation in the SCRJ exhaust gas expansion are used to screen the candidates. Then, the transport similarity parameters (such as Reynolds, Prandtl, and Schmidt numbers) are used to further narrow the choices of substitute gas components. Subsequently, the specific initial temperature and pressure conditions and fractional composition of the substitute gases that exhibit the best pressure distribution match to the SCRJ gases along the entire nozzle expansion process are selected, assuming one dimensional isentropic flow and the particular needs or restrictions of the testing technique to be used. Finally, the best matches of the one dimensional computations are confirmed by two dimensional analysis.

As a result of this procedure we have concluded that binary mixtures of four Freon compounds (Freon 12, 13, 13B1, and 14) with argon additive are good substitutes for SCRJ combustion gases for facility testing of model exhaust nozzles at conditions simulating flight between Mach 4 and 10. Using these

mixtures with about $\frac{1}{8}$ scale models provides complete dynamic inviscid simulation of the flow field pressure distribution along the SCRJ nozzle walls and will closely approximate transport similitude as well. These mixtures are compatible with either the wind tunnel or the detonation tube test facilities.

Similitude Parameters

The nondimensional parameter requirements for dynamic similarity of models in fluid dynamic systems without heat transfer and chemical reactions have been well developed in the literature (e.g., Ref. 2). For inviscid, two or three dimensional compressible flow and geometrically similar systems, the Mach number of the model and prototype must be reproduced throughout the flows so that geometric relationships between physical surfaces and the characteristic directions of propagation in the flow are preserved. A primary additional requirement for this geometric preservation in a nozzle exit region is that the ratio of pressures between the external and internal flows is established such that all wave systems that affect regions of measurement are properly reproduced. In most cases this means a simple matching of pressure ratio, but in some situations corrections for gas thermodynamics are required. If the region of interest is restricted to that inside the Mach cones from the exit lips and there are no compression waves from the exit lips, it is necessary to ensure only that the external pressure is lower than the corresponding flight external pressure. For perfect gases in equilibrium it is then also necessary and sufficient for inviscid simulation that the ratio of specific heats, γ, be the same in model test and in prototype flight. However, the gases involved in SCRJ flows show very significant variations in specific heat within the flow, but in the exhaust region of interest they are well represented by the equation of state $P = \rho RT/\mathcal{M}$, where R is the universal gas constant and the molecular weight $\mathcal{M}$ can be regarded as a local constant (see additional discussion below). This type of behavior is referred to as thermally perfect, and our subsequent discussion and analysis will employ that simplification.

We will show below that a thermally perfect gas flow will be dynamically similar to another flow for matched geometries as defined above whenever the local ratio of specific heats, γ, is the same at corresponding geometric points in the two flows and molecular weight changes along the streamlines of each flow are negligible. Because temperature levels in the two flows

(model and prototype) may be radically different, the proper way to ensure this match is to ensure that $\gamma(T/T_{ref})$ is the same function for both gases, where T_{ref} is the temperature at any convenient geometric reference point common to the two flows. We have chosen the combustor exit plane temperature, T_3, as our reference temperature. The γ function used here is the local ratio of specific heats, c_p/c_v, which should not be confused with the isentropic exponent or the effective γ that can be used to characterize a shock or other finite property change of a process. These latter effective γ's characterize a process in terms of an equivalent process for which the local specific heat ratio would be unchanging, while the γ we use changes throughout the flows. We will henceforth use γ only to characterize relationships among gas properties at a point or for infinitesimal processes, not across finite state changes. For finite processes we will use $\bar{\gamma}$.

The flows of greatest concern in SCRJ simulation are either locally isentropic, or include shock processes. Starting with the shock case, we can write the Rankine-Hugoniot equations to relate properties on either side of a shock wave

$$\rho_a V_a = \rho_b V_b$$

$$P_a + \rho_a V_a^2 = P_b + \rho_b V_b^2$$

$$H_a + \tfrac{1}{2} V_a^2 = H_b + \tfrac{1}{2} V_b^2$$

Normalizing all properties by their conditions at the exit plane (subscript 3), the local velocity can be expressed in terms of the local Mach number

$$V = \sqrt{RT_3}\sqrt{\frac{\gamma}{\mathcal{M}}\frac{T}{T_3}}M \quad ,$$

and the total enthalpy is expressed

$$H = \int c_p dT = RT_3 \int \frac{\gamma}{\mathcal{M}(\gamma-1)} d\left(\frac{T}{T_3}\right)$$

The above system of relationships is closed by the equation of state

$$\frac{P}{P_3} = \left(\frac{\rho}{\rho_3}\right) R\left(\frac{m_3}{m}\right)\left(\frac{T}{T_3}\right)$$

so that any property ratio at b is determinable by knowledge of the state a and the functions $\gamma(T/T_3)$ and $m(T/T_3)$. Note that although m is not a function of temperature ratio alone it is in a particular flow system where ρ and T are coupled to a particular relationship.

Similarly, for external flow the continuity constraint equation is set by the geometry and the constraint of constant entropy is added

$$dS = \frac{dE}{T} + \frac{P}{T}\, d\left(\frac{1}{\rho}\right) = 0$$

The internal energy E can be written

$$E = \int c_v dT = RT_3 \int \frac{1}{m(\gamma-1)}\, d\left(\frac{T}{T_3}\right)$$

so we get

$$\frac{\rho_3 RT_3}{P_3} \int \frac{1}{m(\gamma-1)}\, d\left(\frac{T}{T_3}\right) + \int \left(\frac{P}{P_3}\right) d\left(\frac{\rho_3}{\rho}\right) = \text{constant}$$

Thus we see that if the Mach number at the boundaries is everywhere the same, matching of the functions $\gamma(T/T_3)$ and $m(T/T_3)$ is sufficient to ensure that all property ratios (e.g., P/P_3, ρ/ρ_3, etc.) are matched in two different inviscid flows, with or without shock processes.

For the $M_\infty = 10$ flight case we find that with no shock waves present, the equilibrium molecular weight varies from about 24.3 at the combustor exit to 24.6 at the end of the afterbody. Even if the flow were shocked back to the sonic condition, the molecular weight would not go below 22.7. For the $M_\infty = 8$ flight case, the m variations are even less. We have

therefore concluded that the molecular weight can be treated as a constant in the SCRJ exhaust, even in the presence of shocks, and that substitute gases need only have matching γ and Mach number distributions for inviscid similarity. Note again that $\mathcal{M}$ of the substitute gas and SCRJ flow need not be the same.

Inclusion of viscous regions in the similitude requires matching of Reynolds number, Re. Also necessary for dynamic similarity in either the viscid or inviscid case is the similarity of properties of the gas used for model testing and the gas associated with the prototype. Principal inviscid gas properties are represented by Prandtl number, Pr, and the variation of viscosity and thermal conductivity with temperature, where $Pr = c_p \mu k^{-1}$, which can be considered the ratio of momentum diffusion to thermal diffusion.

The viscosity of gases is independent of pressure at relatively low pressure and generally increases with temperature. For nonpolar gas molecules, the viscosity varies as a power of temperature, n, where n approaches 0.5 for high temperature gases and is nearer 1.0 for low temperatures. Polar gases, such as the H_2O which comprises approximately one third of the SCRJ exhaust gas composition, cannot have their viscosity variation so easily characterized. However, over a finite temperature range of interest, the viscosity calculations or data for SCRJ and test gases can be fitted locally by a law such as $\mu_1/\mu_2 = (T_1/T_2)^n$, or by a two-constant Sutherland equation such as $\mu = bT^{3/2}(S + T)^{-1}$, where b and S are constants. In this way the model test and prototype operation conditions can be examined for similarity of the viscosity distributions. Thermal conductivity of gases, k, increases nearly linearly with temperature. However, for diatomic and polyatomic gases no general temperature relation has been found satisfactory. Curve fitting of k to a polynomial in temperature using test or computed data is one way of representing this transport property. The use of Pr as a similarity parameter characterizes the relationship between μ and k, but the relationship is strictly correct only if Pr is invariant with temperature.

In combustion, chemical reactions, and heat transfer processes, four additional independent similarity parameters are necessary. The diffusion of mass from one part of the multispecie system to another must be considered. The Schmidt number, Sc, ratios the diffusion of momentum to mass

$$Sc = \mu\, RT(PD_{12}\mathcal{M})^{-1} \quad .$$

From Sc and Pr the Lewis number, Le, is derived to give the ratio of mass diffusion to thermal diffusion:

$$Le = \frac{Pr}{Sc} = P\mathcal{M}c_p D_{12}(RTk)^{-1} \quad .$$

The first and third Damköhler parameters, D_I and D_{III} also are important, especially in chemically reacting flows. The ratio of residence time of a reacting gas mixture in a flow channel, L/V, to the duration of the controlling chemical reaction, t_i, is given by the first Damköhler grouping, $D_I = L/Vt_i$. For $D_I \gg 1$, the gas can be considered in local equilibrium even though several secondary reaction products may not have reached final concentrations. For $D_I \ll 1$ the reaction products will be nearly frozen in composition during the process. For accurate details of the flow chemical kinetic rate data must be used with the flow equation. In both the SCRJ exhaust gas flow and detonation tube simulator, the kinetics can be important in determining the flow field and pressure distribution for high Mach number (altitude) cases, although the coupling to pressure is rather weak. For the binary substitute gas mixture, the components are chemically unchanging, and the only relevant kinetic process is vibrational relaxation of the polyatomic molecules in the blend. For conditions characteristic of the use of substitute gases (i.e., moderate temperature and near atmospheric pressure), their vibrational relaxation time is on the order of 10^{-8} to 10^{-6} seconds (Ref. 3), which corresponds to vibrational relaxation lengths very much smaller than crucial flow field dimensions along stream tubes. Equilibrium γ values should therefore be valid for substitute gas flows.

If the SCRJ combustor is efficient, the value of D_I at the combustor exit should be of the order of unity because $t_i \simeq 10^{-4}$s for nearly complete energy release in the supersonic diffusion flame (Ref. 4). As the exhaust flow expands, the local temperature and pressure decrease, the reaction rate decreases (or reaction time increases), and $D_I < 1$. This case describes a condition in which an essentially frozen composition experiences the expansion process. The detonation tube gases at the model test section can be tailored to provide the same composition as the flight SCRJ combustor exit condition, but at a much higher pressure to achieve proper scaling. The higher pressure results in

more recombination reactions and tends to defer the onset of freezing. Calculations (Ref. 5) showed that this effect nearly compensates for the high dissociation in the stagnation region of the detonation tube. Although the chemical reaction history is not identical, the detonation tube system provides the closest reproduction of flight chemistry of any available simulation method. For the substitute gases, $D_I >> 1$, and when used in SCRJ simulation facilities, they should always be in a thermodynamic equilibrium condition.

The D_{III} parameter involves the relation of combustion energy release, and the ratio of residence to reaction time (or D_I) to the thermal energy transferred to the working fluid. Examination of the test concepts we propose does not show any significant relevance of D_{III} to the SCRJ simulation process.

The Eckert number is useful in characterizing the heat transferred from the SCRJ exhaust products to the afterbody surface and cowl, and thereby the effect of heat transfer on growth of the boundary layer. This parameter relates the prevailing temperatures of the exhaust products and the boundaries to the heat transferred to the walls, or

$$Ec = \frac{V^2}{c_p \theta}$$

where θ is the temperature difference between the exhaust gas at the outer edge of the boundary layer and the nozzle wall temperature. The SCRJ value for this parameter will not be duplicated directly in the detonation tube, unless the SCRJ wall is cooled to near room temperature, or the model is heated greatly. Fluid dynamic and fluid properties simulation is almost completely reproduced, so Eckert number is reproduced only if wall temperatures are equal. We have concluded that the secondary effect of Ec on pressure distribution does not justify the large expense of heating the model wall and the resultant effects on instrumentation.

In substitute gas flow, the Eckert number can be matched to the SCRJ condition, despite the fact that θ and the heat transfer is much smaller for the relatively cool test mixtures. This is possible because the model test gas velocity and c_p values are each quite different for the SCRJ gases at comparable model stations. Thus, for example, a model wall at room temperature,

using 400°K substitute gas, can match Ec for the SCRJ, where the exhaust gases are over 2000°K.

It should be noted that the usual inviscid heat transfer simulation, which involves only duplicating Nusselt number ($Nu = \dot{q}L(kA\theta)^{-1}$ and geometry, is not adequate for the SCRJ exhaust nozzle process because of the large compressibility effects (i.e., large density changes) as well as viscous dissipation.

Substitute Gases

Substitute gases appear to be the best solution to the conflict between the required thermodynamic behavior in afterbody model testing and the present lack of a method for generating high temperature exhaust gas chemistry and thermodynamics in a wind tunnel test. Low specific heat ratio, γ, gases have been used with success for simulating high temperature air flows in hypersonic testing (e.g., Refs. 1, 6, and 7), and those experiences were the initial stimulus to their application in SCRJ simulation. Typical candidates for these substitute gases are several Freon compounds and sulfur hexafluoride (SF_6) that can be used at moderate operating temperatures and pressures in a wind tunnel for supersonic speeds and are chemically stable over a wide temperature range. However, some of the best Freon compounds and SF_6 require too low a temperature to duplicate the specific heat ratio of SCRJ gases at the entrance of the exhaust nozzle, and, consequently, they experience phase change (condensation) along the expansion process. This undesirable test gas property can be overcome by fractional additives of high specific heat ratio, stable noble gases, such as argon. We thereby create binary and ternary mixtures capable of matching the ratios of thermodynamic properties of virtually any SCRJ high speed flight propulsion system (exemplified by the values of γ of the combustion products). Figure 1 shows the $\gamma(T)$ behavior of several such blends as well as that of the SCRJ exhaust flow in equilibrium. It should be noted that we do not wish to match $\gamma(T)$; instead, we wish to reproduce $\gamma(X)$ at a much lower temperature level, which can be viewed in the previous context as matching $\gamma(T/T_3)$.

Thus, by selection of appropriate and convenient working temperature, pressure, and binary gas mixture composition, the SCRJ exhaust distributions of γ, M, and Re can be matched in a test facility using small scale models. Furthermore, the different working requirements of different test techniques can be

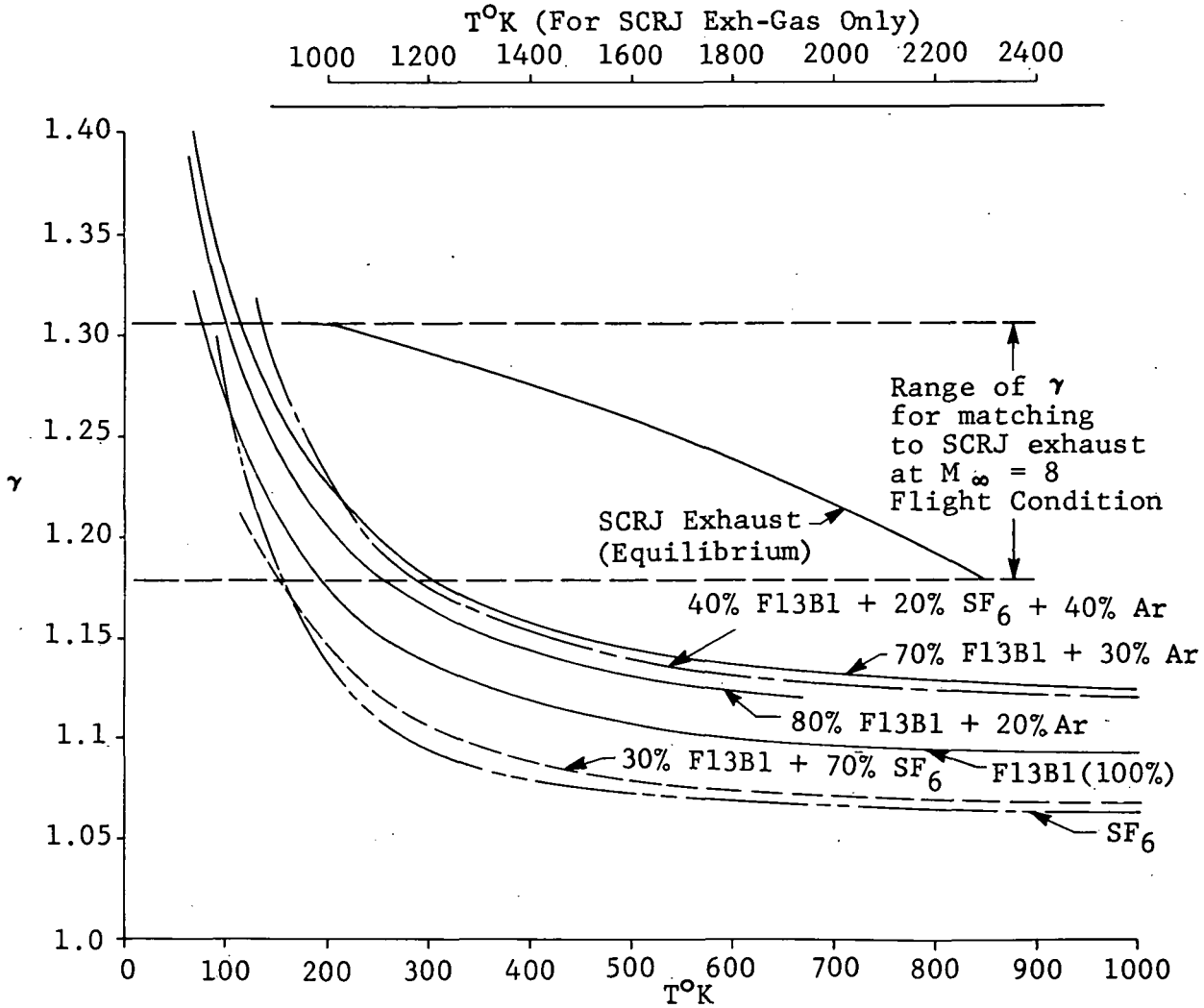

Fig. 1 Variation of γ with Temperature for SCRJ Exhaust and Substitute Gas Formulations

accommodated. Figure 2 presents curves of how changes in composition affect the temperature at which there is an exact match to γ and M at the exit for flight conditions of $M_\infty = 8$, 6, and 4; an effective angle of attack $(\alpha + \beta)$ of 4°; and equivalence ratios (ϕ) of 1.0, 1.0, and 0.6, respectively. These representative trends are for binary mixtures of Freon 12, 13, 13B1, and 14 with argon additive and can readily be extended to match requirements of other flight conditions or for other matching points in the flow.

Table 1 compares several similarity parameters and thermodynamic and transport properties of a $M_\infty = 8$ SCRJ operational condition with two typical substitute gas mixtures of Freon 12 and 13B1 with argon additive. Figure 3 shows that these mixtures are designed to produce the best pressure distribution match to the 1-D computed SCRJ exhaust gas along the nozzle walls. Small compositional changes in the selected substitute gas mixture can result in significantly lower stagnation temperature requirements, with relatively minor alteration in pressure distribution match. Other flight Mach numbers can also be matched similarly. It is necessary to prevent the Freon component gas from condensing within the model flow field. To illustrate this point, the required 622 K stagnation temperature for the 50 percent Freon 13B1 + 50 percent Argon mixture (see Table 1) can be lowered to 485 K by changing to a 58 percent Freon 13B1 & 42 percent Argon mixture. The Freon fraction then will still be well within the vapor phase — a static temperature of 185 K and partial pressure of 4500 Newton/m^2 (0.653 psia) — for Mach 4.06 flow at the end of the model afterbody. The 22 percent lower stagnation temperature can be extremely effective in simplifying the utilization of existing wind tunnels. Computational methods are described in the appendix. Subsequent calculations discussed in the Two Dimensional Afterbody Pressure and Force Predictions section will show how two-dimensional calculations using the same substitute gas behavior compare to the SCRJ case.

The SCRJ exhaust gas properties and similarity parameters are obtained from the standard NASA Lewis Research Center Computer Program (Ref. 8) for an equilibrium kinetics expansion process of hydrogen/air reaction products. The program results are augmented by our additional calculations of Sc and Le, which use a mutual diffusivity value computed for the SCRJ exhaust gases. This value was obtained by assuming that the

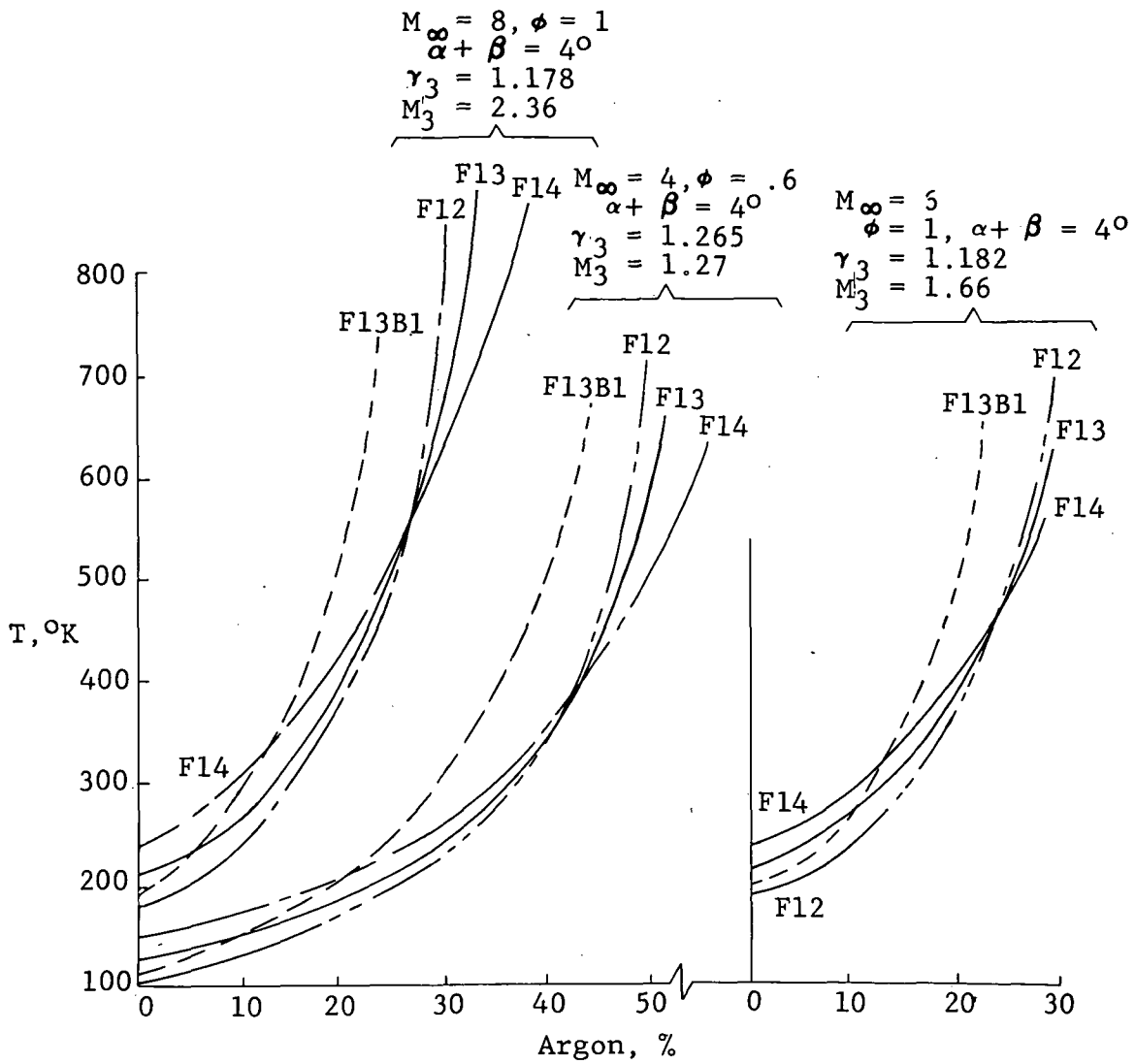

Fig. 2 Composition-Temperature Requirements for Binary Gas Mixtures to Simulate SCRJ Nozzle Entrance Gas Conditions

TABLE 1

SOME PROPERTIES OF SCRJ EXHAUST GAS AND POSSIBLE SUBSTITUTE GAS MIXTURES

Parameter	Hydrogen-Fueled SCRJ at Comb. Chamber Exit $M_\infty = 8$, $\alpha+\beta = 4°$, $\phi = 1.0$	Substitute Gas Mixtures	
		50% Freon 13B1 + 50% Argon	40% Freon 12 + 60% Argon
Mach No.: M	2.36	2.36	2.36
Reynolds No.: Re	6.614×10^5	$6.614 \times 10^{5\dagger}$	$6.614 \times 10^{5\dagger}$
Ratio of Specific Heats: γ	1.178	1.1994	1.224
Reynolds No./Meter: Re/m	2.17×10^6	1.74×10^7	1.74×10^7
Prandtl No.: Pr	0.5289	0.7466	0.708
Schmidt No.: Sc	5.02	4.08	4.46
Lewis No.: Le	0.105	0.183	0.158
Molecular Weight: $\mathcal{M}$	24.40	94.42	72.324
Static Pressure: P, N/m^2	5.516×10^4	2.837×10^4	2.95×10^4
Total Pressure: P_o, N/m^2	8.309×10^5	5.132×10^5	4.69×10^5
Static Temperature: T, °K	2305.0	400.0	400.0
Total Temperature: T_o, °K	3164.0	622.0	649.0
Velocity: V, m/sec	2272.5	485.0	564.0
Viscosity: μ, 10^{-6} gm/sec-cm	735.0	230.0	210.0
Thermal Conductivity: k, 10^{-6} cal/cm-sec-°K	883.0	38.5	41.3
Specific Heat for Constant Pressure: c_p, cal/gm-°K	0.635	0.1258	0.1398
Exponent of Viscosity-Temperature Power Law Approximation: n	$\sim$ 0.73	0.82	0.81

†Matched for $\frac{1}{8}$-Scale Model

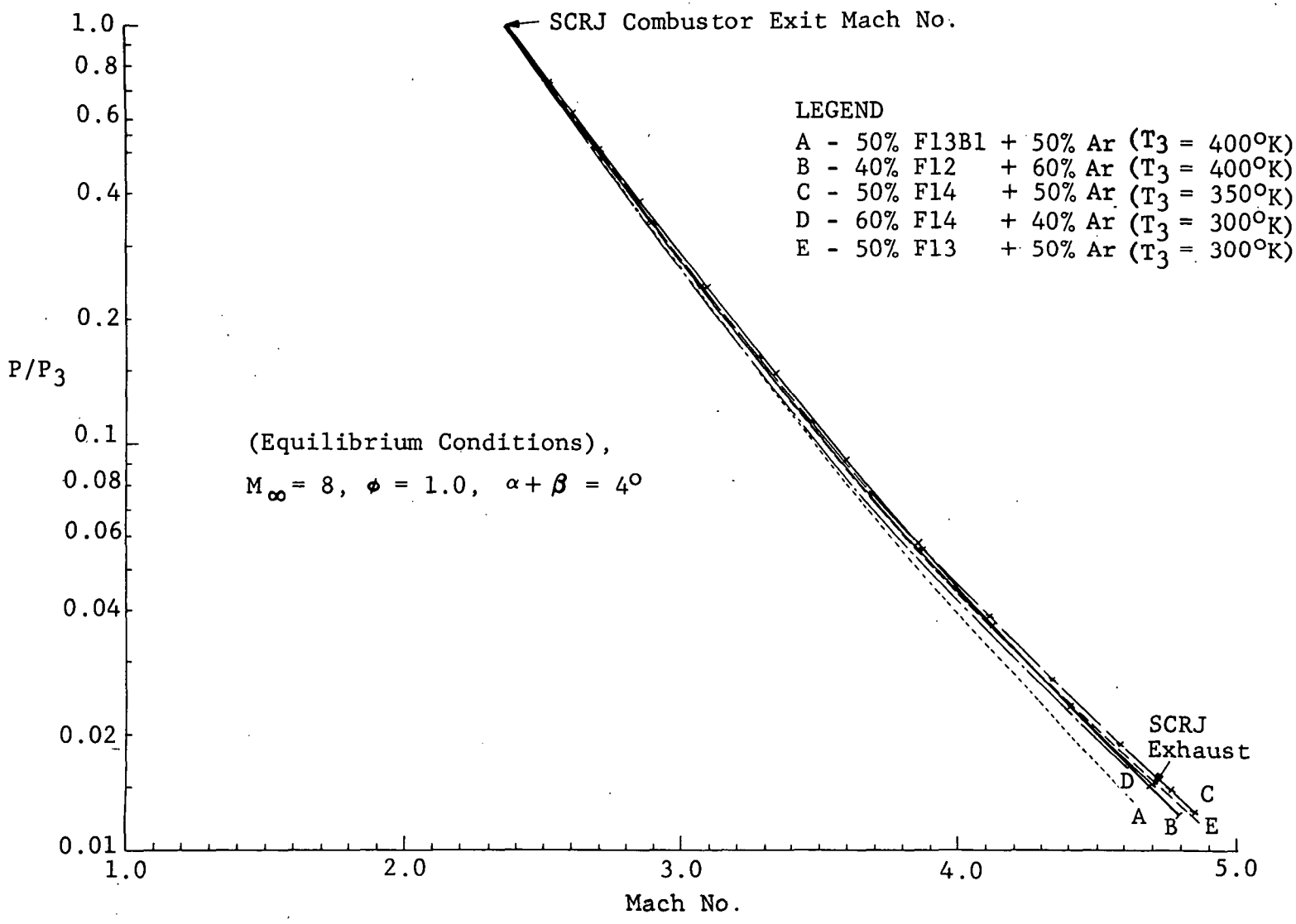

Fig. 3 Preliminary Match of SCRJ Exhaust Pressure Distribution with Five Substitute Gas Expansions

principal SCRJ exhaust components of N_2 and H_2O can be approximated as a binary mixture. Calculations of the substitute gas properties and parameters are described in the appendix.

The properties of the two substitute gas flows shown in Table 1 were established by matching the Mach number and Reynolds number exactly for the conditions at the combustor exit of a $\frac{1}{8}$ the scale model once the gas blends were chosen. The gas flows were all assumed to be homogeneous. The initial γ of each of the substitute gases is larger than that of the SCRJ, but these selected binary mixtures produce nearly the same over-all pressure distribution as the SCRJ along the nozzle expansion. As was shown in Fig. 1, the γ versus T trends of the SCRJ gas and substitute test gases are not identical; however, it is possible for the latter to reproduce the working range of γ for the SCRJ, but at much lower temperatures. As shown by Fig. 3, the matching of the different substitute gas isentropes to the SCRJ expansion pressure distributions is very close.

In preliminary selection of substitute gas candidates, the best similarity parameter to be used is the value of $\bar{\gamma}$ characterizing the over-all expansion process. For isentropic expansion of the chemically nonreactive substitute gas mixtures, considered as a perfect gas, the process-averaged $\bar{\gamma}$ is the isentropic exponent of the relation $(P/\rho)^{\bar{\gamma}} = \text{constant}$. Then

$$\bar{\gamma} = \frac{\log\,(P_2/P_1)}{\log\,(\rho_2/\rho_1)} = \frac{\log\,(P_2/P_1)}{\log\,(P_2/P_1) - \log\,(T_2/T_1)}$$

where the subscripts 1 and 2 refer to the nozzle entrance and exit conditions, respectively. For the three candidate substitute gas compositions whose gas dynamic properties are given by Table A-1 (see p. 68), the $\bar{\gamma}$ for the nozzle expansion process (between Mach numbers 2.36 to 4.06) is as follows:

50 percent Freon 13B1 + 50 percent Argon - $\bar{\gamma} = 1.24$

40 percent Freon 12 + 60 percent Argon - $\bar{\gamma} = 1.27$

58 percent Freon 13B1 + 42 percent Argon - $\bar{\gamma} = 1.20$

The expansion of SCRJ gases involves small changes in equilibrium chemical composition leading to slight changes in molecular weight dependent on the local pressure and temperature. In this polytropic process, the process-averaged exponent, $\bar{\gamma}^c$, governing

the $(P/\rho)^{\overline{\gamma}^c}$ relation is now defined as

$$\overline{\gamma}^c = \frac{\log (P_2/P_1)}{\log (P_2/P_1) - \log (T_2 m_1/T_1 m_2)}$$

to account for the molecular weight changes. From the equilibrium gas dynamic data generated by the method of Ref. 8 for the $M_\infty = 8$, $\alpha + \beta = 4$, $\varphi = 1.0$ SCRJ operational condition, the value of $\overline{\gamma}^c$ equals 1.24. For the frozen composition SCRJ gas dynamic properties the value of $\overline{\gamma}$ is calculated by the same relation as for the substitute gases, and for the $M_\infty = 8$ SCRJ condition has a value of 1.277. From data shown in Fig. 16 it will be seen that the resulting forces produced by the SCRJ pressure distribution along the nozzle surface is nearly exactly simulated by substitute gas expansions where $\overline{\gamma}$ is very nearly equal to $\overline{\gamma}^c$, in the SCRJ equilibrium case, and where the $\overline{\gamma}$'s are equal for the frozen SCRJ case. Note again that the purpose of $\overline{\gamma}$ is only for preliminary selection; the actual $\gamma(T/T_3)$ function for the substitute gas must be used in a multidimensional calculation before it can be accepted as a valid substitute gas.

Other similarity trends shown by the data of Table 1 are:

- Prandtl No. The low value ($Pr \sim 0.50$) for the SCRJ exhaust shows that thermal diffusion is stronger than momentum diffusion. The substitute gas selections will have a somewhat less dominant thermal diffusion process, being more like the familiar levels of low temperature air. In this regard, the Freon 12 and argon mixture is a better simulation than the Freon 13B1-argon composition. Note that Pr is not changed significantly by pressure changes, nor does a change in Pr have a large effect on pressure distribution in nearly adiabatic attached flows.

- Schmidt No. In view of the large Sc value for both the SCRJ and the substitute gases, the mass diffusion in each case is $\frac{1}{4}$ to $\frac{1}{5}$ of the diffusion of momentum in the flow field. All cases are comparable although the Freon 12 + argon component mixture is a slightly better match to the SCRJ case.

- Lewis No. The very low value of the SCRJ and substitute gases indicates that in both situations, the diffusion of the temperature field is almost an order of magnitude greater than mass diffusion.

As previously discussed, dynamic similarity requires simulation of gas properties; for detailed nozzle boundary layer development the simulation of transport property variation with temperature is of great importance because of the large temperature gradients in the gas adjacent to the nozzle wall. While the Reynolds number matching of model and SCRJ governs the overall flow process, the boundary layer bears special consideration because of its possibly significant interaction with the flow field pressure distribution. The viscosities of the binary substitute gas mixtures listed in Table 1 are about one third that of the SCRJ exhaust gas at the nozzle entrance. This reflects primarily the large difference in temperature of the two working fluids.

Perhaps of greater significance is the temperature variation of viscosity of the substitute gases compared to the SCRJ gases in their respective temperature ranges of operation as shown by Fig. 4. This variation can be characterized by the value of the exponent, n, in a power law approximation of μ versus T. As shown in Table 1, the n value for the binary substitute gases is about 10-12 percent larger than the SCRJ gases.

It is well-known that the viscosity-temperature exponent will have a greater effect on boundary layer growth and related parameters at supersonic Mach number than will relatively large changes in Pr. Because the inviscid similitude laws provide a correspondence in temperature ratios between corresponding adiabatic points in substitute and SCRJ flows [i.e., (T_2/T_1) substitute gas $\tilde{}$ (T_2/T_1) SCRJ], we can establish reference viscosity ratios for the afterbody boundary layer characterized by adiabatic temperature levels — say, stream and stagnation temperature. These will ensure corresponding viscosity distributions in the wall cooling (Eckert number) are all the same. It is our feeling that the matches of n and Pr shown in Table 1 are more than adequate for their relatively weak coupling to pressure distribution, but the final test of this opinion will come when substitute gases are tested against detonation tube SCRJ flows in Phase II of this program.

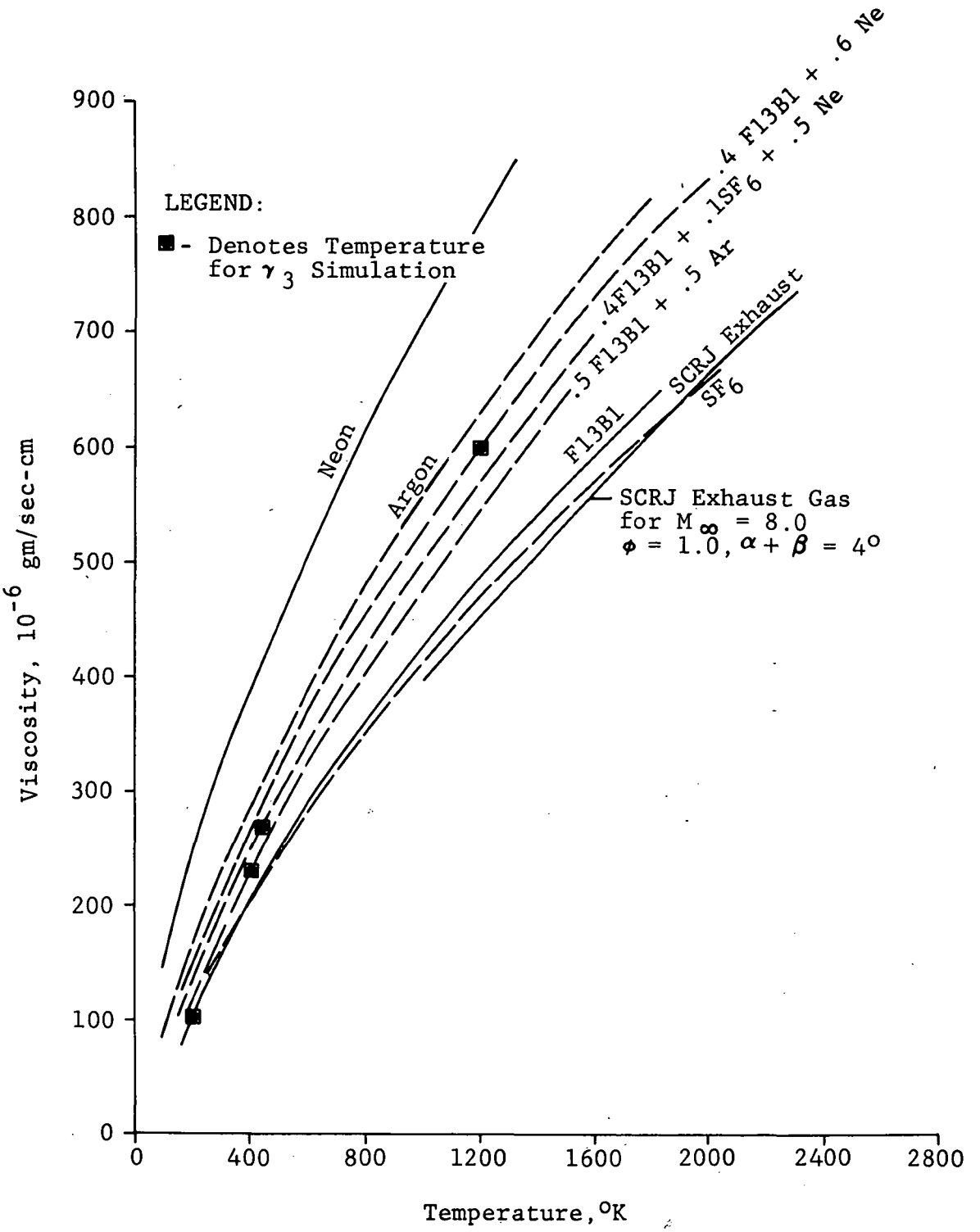

Fig. 4 Temperature Variation of Viscosity for SCRJ Exhaust Gas and Several Substitute Gas Compositions

The viscosity properties of a ternary mixture are also shown by Fig. 4 where a Freon 13B1-sulfur hexafluoride-neon mixture formulation is plotted.

The ternary mixture was examined to see if its $\gamma(T)$ variation would prove superior to the best binary mixtures, or if there were significant advantages in the transport properties of the ternary mixture. The limited data we generated on ternary mixtures did not indicate any significant advantage for them; in fact the $\mu \sim T$ exponent moved further from that of the SCRJ exhaust gas.

A slightly better (i.e., lower) value of n could be achieved by using a substitute gas mixture of Ne and Freon 13B1 at a stagnation temperature of about 1600 K. While this could be easily done in a shock tunnel, it would create operational difficulty and expense in the subsequent wind tunnel testing that would preclude its selection.

In summary, the distribution of transport property effects in the SCRJ exhaust and binary mixture substitute test gases follow the same relative order of dominance, namely

$$\text{thermal} > \text{momentum} > \text{mass} \quad ,$$

and very similar viscous aerodynamic behavior should be encountered within each working medium.

Mixing Layer Similitude

Complete SCRJ exhaust simulation eventually will involve the mixing of simulated exhaust and external flow fields. The scaling laws for turbulent mixing are not known reliably, so either all of the suspected important scaling parameters must be matched or an experimental investigation must be designed in which any imperfect matching can be varied and evaluated for its effect. The major mixing similitude parameters are: Re, initial boundary layer properties on the internal and external surfaces (perhaps scaled to the inviscid flow properties), and the ratios of internal to external density, velocity, viscosity, and temperature. For inviscid similitude, a simple analysis indicates that the parameter $(T_i/T_e)\ (\mathcal{M}_e/\mathcal{M}_i)$, where $\mathcal{M}$ is molecular weight, will simulate some of these mixing properties if maintained equal in the model and prototype. (The subscripts i and e refer to internal and external flows, respectively.)

For example, the density ratio across the mixing layer is:

$$\frac{\rho_i}{\rho_e} = \left(\frac{P_i}{P_e}\right)\left(\frac{T_e}{T_i}\right)\left(\frac{\mathcal{M}_i}{\mathcal{M}_e}\right)$$

and the velocity ratio is:

$$\frac{V_i}{V_e} = \left(\frac{M_i}{M_e}\right)\left(\frac{\gamma_i T_i \mathcal{M}_e}{\gamma_e T_e \mathcal{M}_i}\right)^{\frac{1}{2}} .$$

For the SCRJ, the magnitude of the parameter $(T_i/T_e)(\mathcal{M}_e/\mathcal{M}_i)$ at the cowl lip is approximately 8.5. This value should be matched in the detonation tube simulator tests and in wind tunnel tests where relatively low temperature substitute gases are used.

For the detonation tube, the ratio $(T_i/\mathcal{M}_i)$ is about 80 so the required $(T_e/\mathcal{M}_e)$ ratio is about 9.5 for exact matching. This condition is easily obtained by using air $(\mathcal{M}_e = 29)$ for the external flow, and setting test conditions to produce a T_e of about 275 K at the cowl lip station.

For the wind tunnel test situation, the types of substitute gases selected for SCRJ internal flow simulation give a $(T_i/\mathcal{M}_i)$ ratio of 3.7 to 4.7. This establishes a $(T_e/\mathcal{M}_e)$ ratio requirement of 0.43 to 0.55 for the external flow substitute gas. For the safe Freon compounds and binary mixtures considered for SCRJ exhaust gas simulation, the molecular weight will be in the range of 70 to 150. If used as an external gas, this would result in a need for extremely low temperature, T_e (on the order of 50 K to 100 K), at the cowl lip location with its accompanying danger of phase change for the Freon component at practical pressure levels. To obtain more practical temperature and pressure levels a different class of fluorocarbons is needed. A preliminary survey of safe, chemically stable candidates for this purpose indicates that the Freon "E" series of high molecular weight, low γ, compounds, with $(T_e/\mathcal{M}_e)$ values of 0.52 to 0.72 at their boiling points could be useful components of a binary mixture with high molecular weight noble gases. Freon E5, for example, has a molecular weight of 950 and a boiling point, at atmospheric pressure, of 497 K. Using these "E" series fluorinated ethers at lower pressures than atmospheric could reduce the temperature requirements and decrease the $(T_e/\mathcal{M}_e)$ ratio to the full extent needed to examine mixing processes in wind tunnels. Clearly, this problem requires more extensive study which

could be pursued in the context of a research program concerned with mixing phenomena of high speed parallel flows of dissimilar gases. Also requiring further consideration are the methods and costs of implementation by which the external and internal flows can be supplied and sequenced in short duration tests in both the wind tunnel and detonation tube simulator test techniques. However, a conceptual solution for substitute gas simulation of SCRJ mixing processes appears available within the framework of present technology.

DETONATION TUBE SIMULATOR

The Grumman detonation tube simulator to be used for the measurement of exhaust flows and validation of the substitute gases is capable of giving nearly correct chemistry and total enthalpy for the hydrogen/air combustion system throughout the entire proposed flight regime. Reynolds numbers can easily be maintained at flight values by running at elevated pressures with both combustion and substitute gases. Comparisons of pressure distributions over a model afterbody obtained with the combustion gases against those obtained with candidate substitute gases will be used to select the proper substitute gas and operating conditions for subsequent wind tunnel tests so that the necessary dynamic similitude prevails.

A schematic of the detonation tube facility is shown in Fig. 5. It consists of a 6.1 meter long, 7.62 cm inside diameter driver section initially separated from a 10 meter long, 12.7 cm inside diameter driven tube by a metallic diaphragm. The driven tube is terminated by a supersonic nozzle designed to produce a flow that will match the expected exit plane conditions of the proposed scramjet engine. The nozzle exhausts into a 1.83 meter diameter, 3.66 meter long test section. Mounted within the section, and mating to the supersonic nozzle is the model afterbody. For the proof-of-concept experiments, the upper afterbody surface will be a flat plate instrumented with up to 20 pressure transducers. The test section can be evacuated prior to a run to any desired pressure down to 5×10^{-5} torr. The facility has been designed to handle combustible hydrogen mixtures safely. Various interlocks and leak detection devices are incorporated into the automatic gas handling system. Details of this system may be found in Ref. 1.

The facility has available up to 35 channels to carry model data. All data are recorded through FM/FM multiplexing on magnetic tape and reduced by a special off-line computer. Heat transfer rates are measured using thin film platinum resistance gauges. Pressures in the past have been measured with standard piezoelectric gauges for pressures above 7000 N/m^2 or with special Grumman designed gauges for low pressure work. For the afterbody pressure measurements above 7000 N/m^2 we intend to use a new system using unbonded semiconductor strain gauges. Those are much lower impedance devices than the piezoelectric type and will lead to much less mechanical noise. These instruments use a bridge circuit; differential amplifiers can therefore

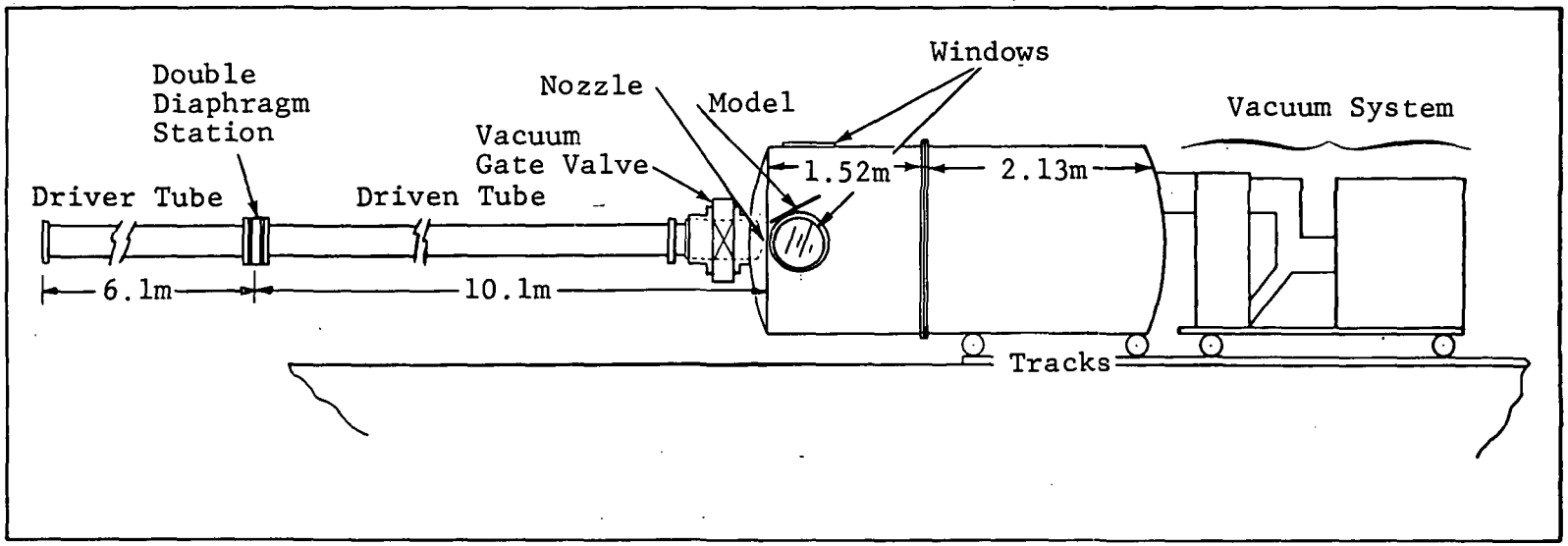

Fig. 5 Detonation Tube Simulator Schematic

be used which will allow the elimination of common-mode noise. Other facility induced noise problems will be unknown until we actually try the system. Since capability for accurate pressure measurement is critical to the successful conclusion of the next phase of the program, we are devoting considerable effort outside the coverage of this contract to achieving the maximum instrument capability possible. For pressures above 7000 N/m^2, gauges are available with sufficient frequency response and with accuracy to $\frac{1}{4}$ of one percent of full scale. In the pressure range from 70 N/m^2 to 7000 N/m^2 we are currently investigating the use of microphone-type gauges to obtain similar accuracies.

Photographic coverage available includes time-exposure glow photographs in color or black and white, high speed movies, and, where there is sufficient density, schlieren photographs. We hope that the schlieren photographs will be sufficiently sensitive to measure relative boundary layer growth in substitute gas and detonation tube tests.

Two modes of detonation tube operation are possible. In the first, called the incident or forward-running detonation technique (Ref. 9), the driver section is pressurized with helium to a pressure high enough to insure detonation of the combustible gases when the main diaphragm ruptures. The diaphragm is scribed to a predetermined depth so that it will rupture at a specific pressure. The shock wave formed will rapidly become a self-propagating detonation wave that will reflect from the nozzle end of the driven tube as a shock wave. The gas is heated and pressurized by the combustion behind the detonation wave and further by the energy addition behind the reflected shock wave. A weak diaphragm at the entrance to the nozzle is ruptured by the arrival of the incident wave and the high energy slug of gas expands through the nozzle into the test section. In order to prevent the rapid expansion that exists behind a free-running detonation wave, the initial helium driver gas pressure is chosen so that when it expands after the rupture of the diaphragm its pressure matches that immediately behind the detonation wave. This produces quasi-steady flow conditions for two to four milliseconds.

The second mode of operation is called the backward-running detonation technique. This technique was developed specifically for the simulation of hydrogen/oxygen rocket engine plumes (Ref. 1) where the incident technique would have produced an enthalpy higher than the actual engine case because of the shock wave heating added to the heat of combustion. A very weak shock wave is sent into the combustible mixture in this method (through the use of a low driver

pressure and weak main diaphragm). The idea is to prevent ignition on the incident wave, but have the gas ignite when the incident wave reaches the nozzle end of the tube. The detonation wave then travels away from the nozzle back towards the driver section. The expansion following this wave drops the pressure and enthalpy in the test gas, which then expands through the nozzle. We have found in previous work (Ref. 1) that the ignition at the end of the tube is best accomplished by a timed electrical spark, although under certain conditions spontaneous ignition behind the reflected wave will occur.

The choice of technique to be used for the scramjet simulation depends on the final conditions required and to some extent on operational experience during exploratory tests to be made during the next phase of this program. Further discussion of this choice is given in the next section where calculated running conditions for various mixtures are presented.

For running the inert substitute gases in the detonation tube we run the facility as a conventional reflected shock tunnel. That is, the test gas mixture is placed in the driven tube. Helium driver gas is used. The shock wave formed on rupture of the main diaphragm reflects from the nozzle end of the driven tube to produce a slug of high energy gas which expands through the nozzle into the test section. The stagnation conditions of the substitute gas are determined by the strength of the incident shock wave in the driven tube, which may be easily controlled.

Detonation Tube Simulator Running Conditions

We have been able to show that by the use of one of our two detonation tube techniques we will be able to simulate the HRA exhaust nozzle flow with exact total enthalpy (flight and combustion), full scale Reynolds number, and nearly exact chemistry (exact elemental composition, with nearly exact molecular composition). Calculations were made for the three basic flight conditions specified in NASA Langley Statement of Work 1-53-3387, March 12, 1973, plus the $M_\infty = 8$ flight conditions. It appears at this stage that the detonation tube techniques will give exact total enthalpy simulation only up to $M_\infty = 10$ at $\Phi = 1$, but close simulation is available to higher flight Mach numbers. In the following pages we give some details of the calculations which show the broad range of simulation capability of the detonation tube and how the above mentioned flight conditions fall within our operating range.

Total Enthalpy and Chemical Composition

With the backward-running detonation tube technique we can give exact total enthalpy and equilibrium chemical composition simulation for $M_\infty = 4$ at $\phi = 0.6$, $M_\infty = 6$ at $\phi = 1$, and we may use this method as high as $M_\infty = 8$ at $\phi = 1$.

The procedure for determining the tunnel stagnation conditions is as follows (see also Ref. 1). For a given incident wave speed at the end of the tube, the state properties and particle velocity behind the wave are calculated, assuming real-gas thermodynamic properties and frozen composition. The reflected wave is assumed to be a Chapman-Jouguet (C-J) detonation whose initial conditions are the conditions behind the weak incident shock wave. The unsteady expansion from the C-J state to the tunnel stagnation conditions is calculated assuming an isentropic expansion with equilibrium thermodynamic properties. The governing equation for this expansion is $\sigma - U = \text{constant}$, where

$$\sigma \equiv \int_{\rho_{ref}}^{\rho} (a/\rho)_s \, d\rho \quad .$$

For the C-J state, $U \equiv (U_{CJ} - U_2)$, and for the end wall state (Region 5), $U \equiv 0$. The chemical equilibrium program of Ref. 8 is used throughout these calculations.

There are a wide variety of gas mixtures and initial shock wave speeds that we could use to achieve these simulations. Mixtures would consist basically of H_2, O_2, N_2, and Ar, with various amounts of NH_3 or N_2O added to achieve the desired enthalpy. For $\phi = 0.6$ the gas mixtures could be $(Y)NH_3 + (0.2511 - 3/2\ Y)H_2 + (0.2095)O_2 + (0.7809 - 1/2\ Y)N_2 + (0.0096)Ar$ with $0 \leq Y \leq 0.1674$, or they could be $(X)N_2O + (0.2511)H_2 + (0.2095 - 1/2\ X)O_2 + (0.7809 - X)N_2 + (0.0096)Ar$ with $0 \leq X \leq 0.4190$.

For $\phi = 1$ the mixtures could be $(Y)NH_3 + (0.4190 - 3/2\ Y)H_2 + (0.2095)O_2 + (0.7809 - 1/2\ Y)N_2 + (0.0096)Ar$ with $0 \leq Y \leq 0.27933$, or $(X)N_2O + (0.4190)H_2 + (0.2095 - 1/2\ X)O_2 + (0.7809 - X)N_2 + (0.0096)Ar$ with $0 \leq X \leq 0.4190$.

The actual gas mixture used will be chosen for operational convenience in obtaining the desired stagnation pressure, P_5.

Figures 6 and 7 show the variation of total enthalpy with initial shock wave speed for these gas mixtures. The problem of achieving the $M_\infty = 8$ flight case with the backward-running technique occurs because the incident shock wave Mach number must be greater than 2.5 (see Fig. 7). If this high speed causes an incident detonation, we will use the front-running technique to simulate $M_\infty = 8$. The backward-running technique is preferable because it requires a much lower driver gas pressure to achieve the same stagnation pressure. The higher driver pressure required by the front-running technique is due to the high contact surface velocity required to match the pressure behind the detonation wave.

With the front-running detonation tube technique we will be able to achieve exact total enthalpy simulation at $\phi = 1$ from about $M_\infty = 7$ to $M_\infty = 10$, overlapping the conditions simulated by the backward-running technique. For a given gas mixture the forward-running technique generates a higher total enthalpy because the burned gas is further heated by a reflected shock wave, rather than cooled by an expansion wave as with the backward-running technique.

The stagnation conditions for each gas mixture are determined by first calculating the conditions behind the detonation wave assuming the C-J condition (see Ref. 9). The steady flow conservation equations and the equation of state are then applied across the reflected shock wave assuming a constant ratio of specific heat, γ, equal to that behind the detonation wave.

Figure 8 is a graphical presentation of the variation of total enthalpy with the $\phi = 1$ gas mixtures specified at the beginning of this subsection. For a specified total enthalpy, X and Y are only weak functions of the stagnation pressure, P_5, since the initial shock Mach number is now fixed at the predetermined Chapman-Jouguet detonation wave speed for each mixture. It is fortuitous that to simulate $M_\infty = 8$, the flight condition agreed upon for our initial experimental work, no other molecular forms of the elements in the combustion gases are required to be added to the basic H_2/air mixture (see Fig. 8).

Model Size and Reynolds Number

Both the backward-running and forward-running techniques require reflected shock waves. As a general rule, to produce the desired stagnation conditions behind a reflected shock wave, the throat area in the end wall of the shock tube should not exceed

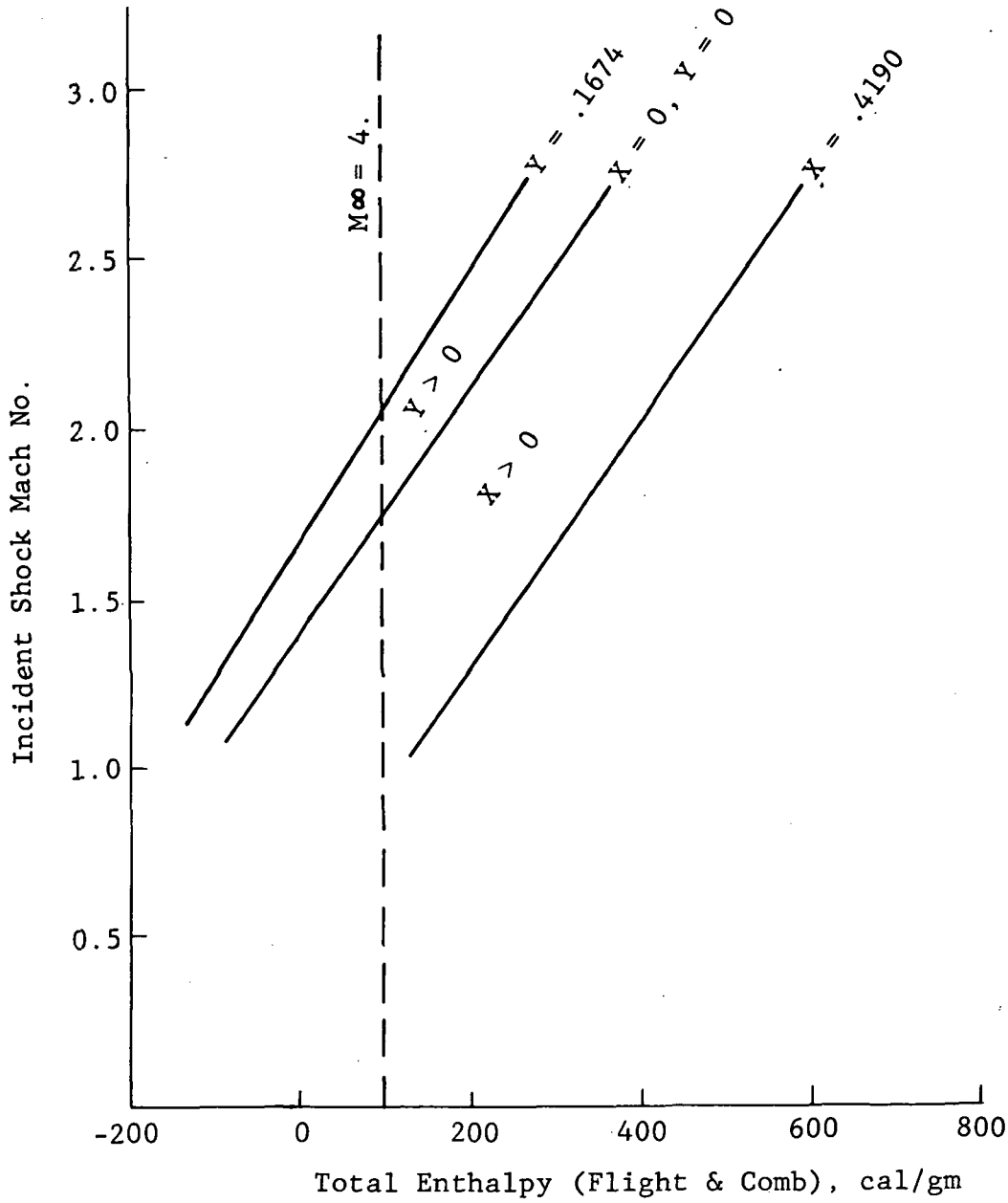

Fig. 6 Backward Running Detonation Tube Total Enthalpy for Various Gas Mixtures for Simulating H_2/Air Scramjet Combustor Exit Conditions at ϕ = 0.6

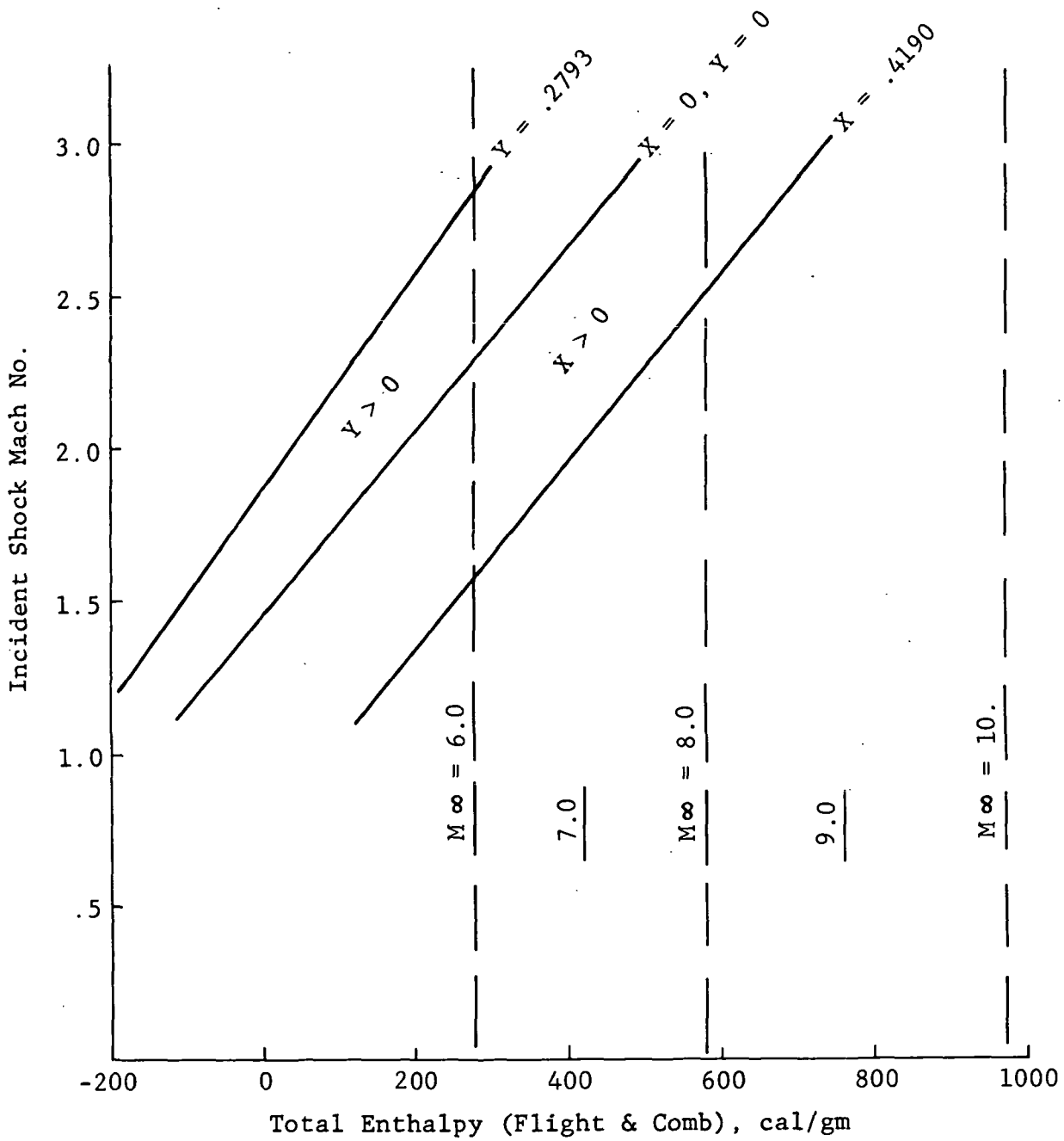

Fig. 7 Backward-Running Detonation Tube Total Enthalpy for Various Gas Mixtures for Simulating H_2/Air Scramjet Combustor Exit Conditions at ϕ = 1.0

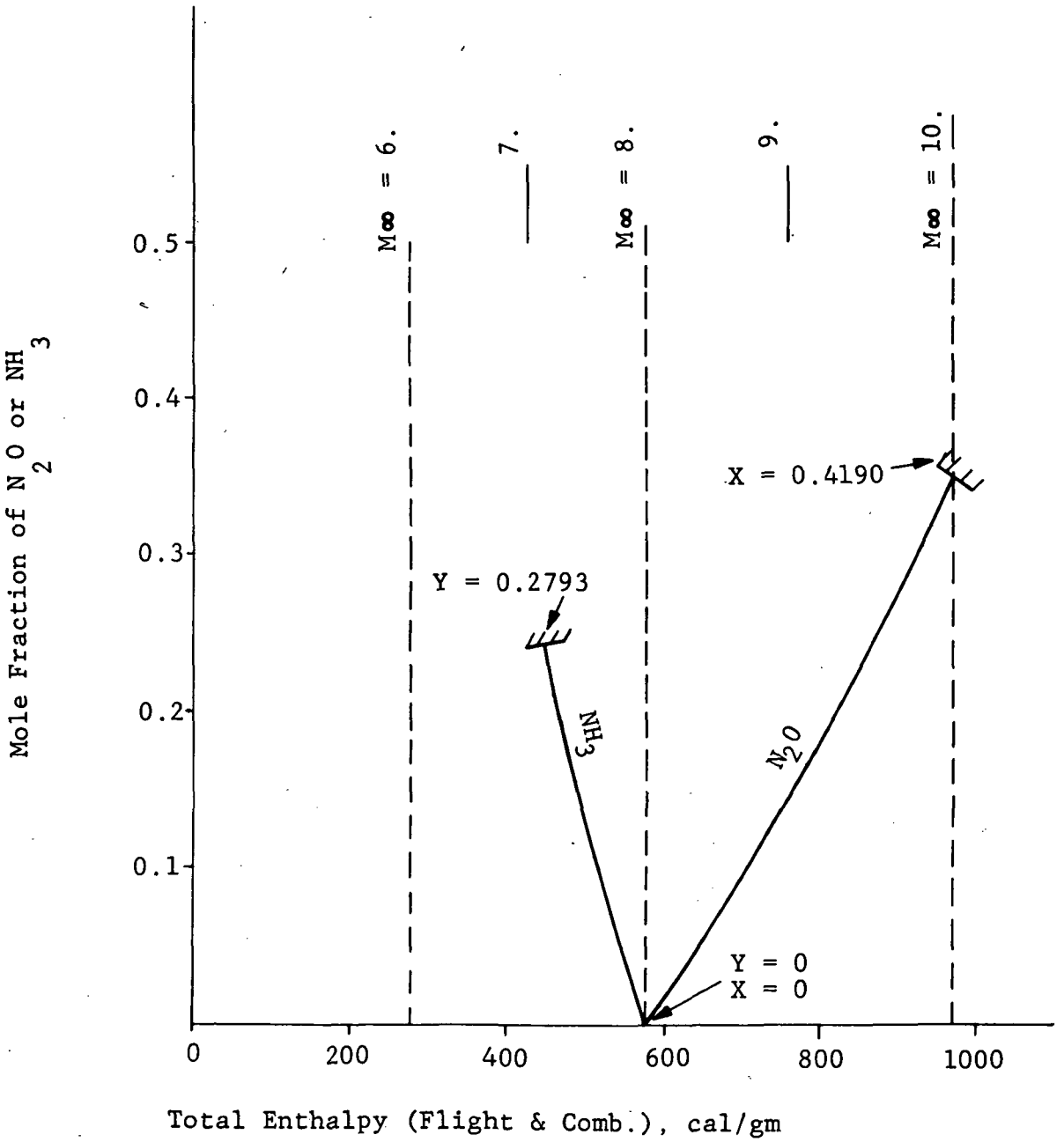

Fig. 8 Forward-Running Detonation Tube Total Enthalpy for Various Gas Mixtures for Simulating H_2/Air Scramjet Combustor Exit Conditions at ϕ = 1.0

10 percent of the shock tube cross section area. The combustor exit plane Mach numbers and shock tube nozzle exit to throat area ratios required to generate those Mach numbers are given below for the cases under consideration.

M_∞	Φ	M_{exit}	Shock Tube A_e/A^*
4	0.6	1.29	1.07
6	1.0	1.68	1.40
8	1.0	2.34	3.10
10	1.0	3.00	8.30

Note: The variation of M_{exit} and A_e/A^* with $\alpha + \beta$ is very small. The above numbers are average values for the 3 $\alpha + \beta$'s at each M_∞.

If we assume a two dimensional combustor with a square exit plane and a throat area A^* equal to one-tenth that of the detonation tube cross section, the maximum exit plane dimensions become:

M_∞	Maximum Exit Plane Dimensions, cm
4	3.683 x 3.683
6	4.318 x 4.318
8	6.1 x 6.1
10	10.16 x 10.16

A rectangular exit plane with an aspect ratio greater than 1 was chosen, primarily because it will give a relatively larger volume of two dimensional flow than the alternatives, giving measurements which could be more easily compared to theory. The $M_\infty = 8$ flight condition was also chosen as the nominal baseline for the first series of experiments required to prove the concept of detonation tube simulation for a SCRJ. In Fig. 9 we show the maximum combustor exit plane dimensions for various aspect ratios for the four flight conditions under consideration. Given

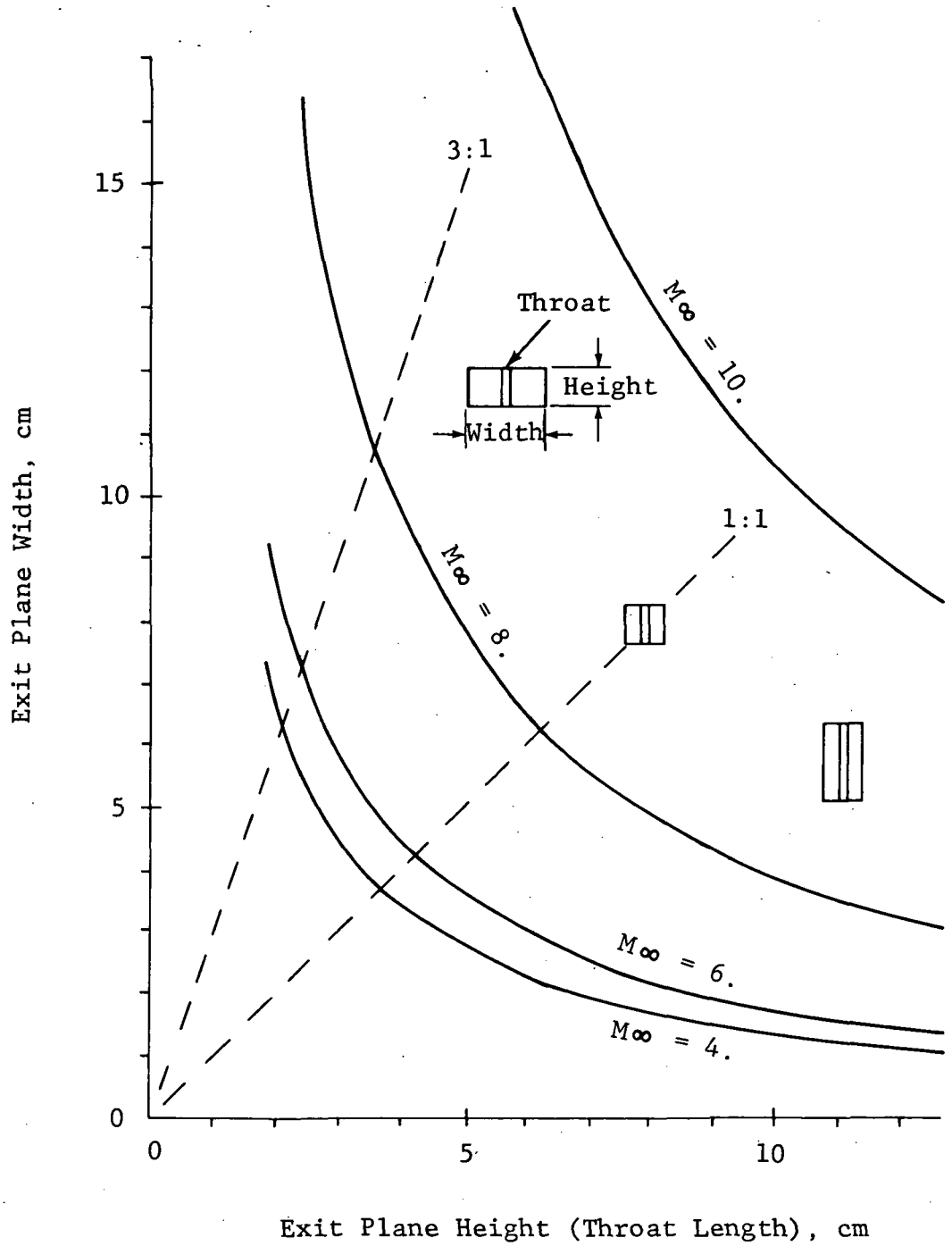

Fig. 9 Maximum Exit Plane Dimensions for 12.7cm Diameter Shock Tube Operation with $A_{throat} = 0.1A_{Det.\ Tube}$

the restraints of a 12.7 cm i.d. detonation tube with throat area one tenth of the detonation tube area and $M_\infty = 8$, we chose a 3:1 aspect ratio for the combustor exit plane with a width of 11.43 cm and a height of 3.81 cm. With the 3.81 cm height we can also fit three 3.81 cm x 3.81 cm square combustor nozzles in the end wall of the detonation tube, thus simulating the 3:1 aspect ratio with and without separators. Figure 10 is a sketch showing the proposed single nozzle arrangement and Fig. 11 shows the same shock tube and afterbody model, but with the three smaller nozzles installed in the detonation tube end wall.

To achieve full scale Reynolds number we first determined the exhaust flow Reynolds number per meter at the prototype combustor exit plane, using the NASA/Lewis computer program (Ref. 8). These results are presented in Table 2. Since we chose a model combustor height of 3.81 cm while the prototype is assumed to be 30.48 cm, we will be doing 1/8 scale testing based on combustor exit height and must achieve in the model combustor a Reynolds number per meter eight times that of the prototype for proper viscous flow development on the afterbody.

To determine the stagnation conditions in the detonation tube that are required to achieve the desired Reynolds number at the model combustor exit, we assumed the following:

1. The total enthalpies of the prototype and model flows are identical.

2. The equivalence ratios of the prototype and model flows are identical.

3. The flow from the detonation tube stagnation region to the model combustor exit is in equilibrium.

4. The combustor exit to sonic throat area ratio in the model (A_3/A^*) is the same as the theoretical combustor exit to sonic throat area ratio in the prototype.

The last assumption required calculating a theoretical sonic condition for the prototype. The differences in exit Mach number, between model and prototype, were on the order of a few hundredths of a Mach number, not enough to justify additional calculations to achieve an exact match. Using these assumptions with the computer program of Ref. 8, we determined the detonation tube stagnation

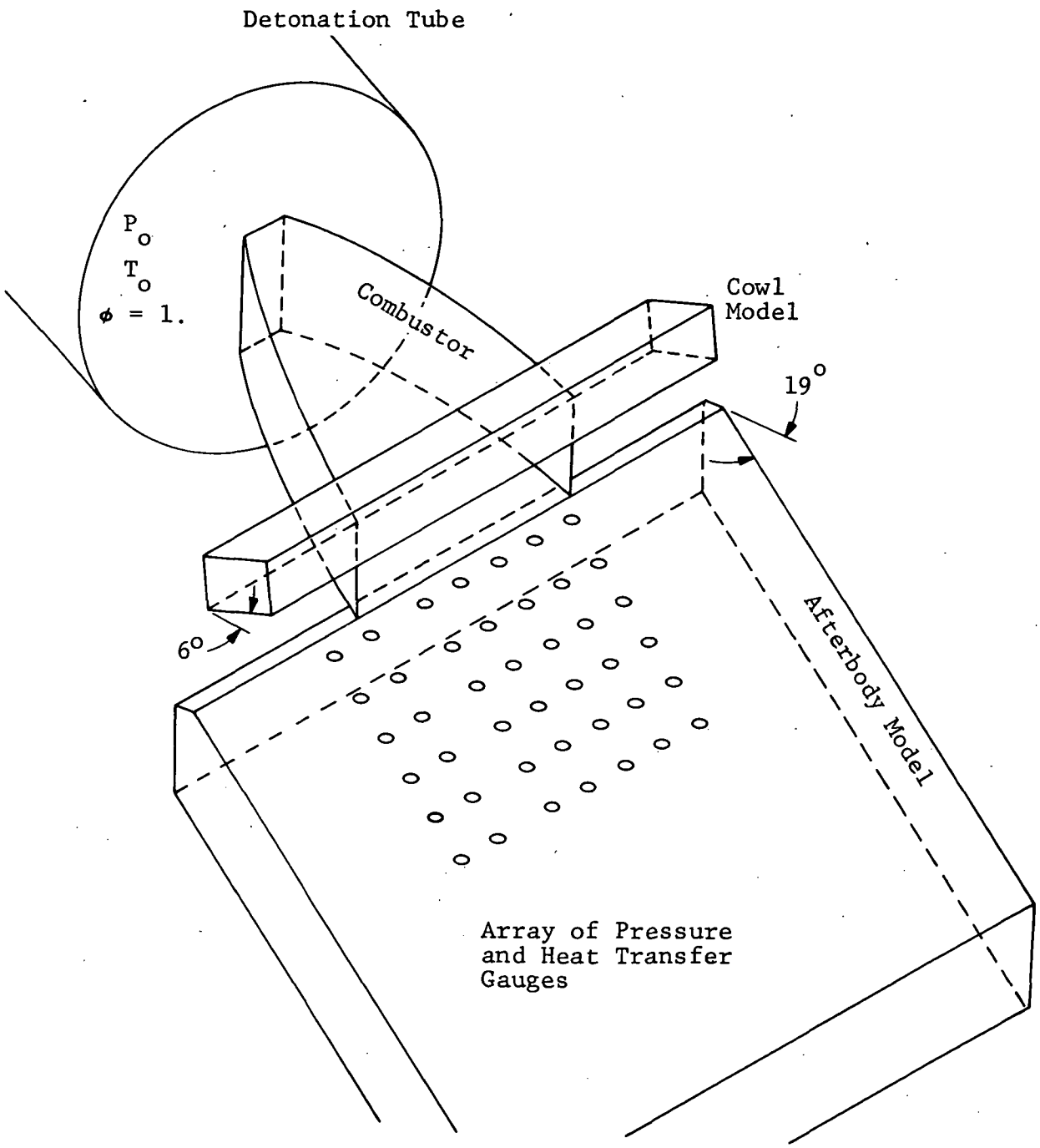

Fig. 10 Sketch of Detonation Tube and Model Installation for Unsegmented, $\mathcal{A}R$ = 3 Scramjet Combustor Exit Plane

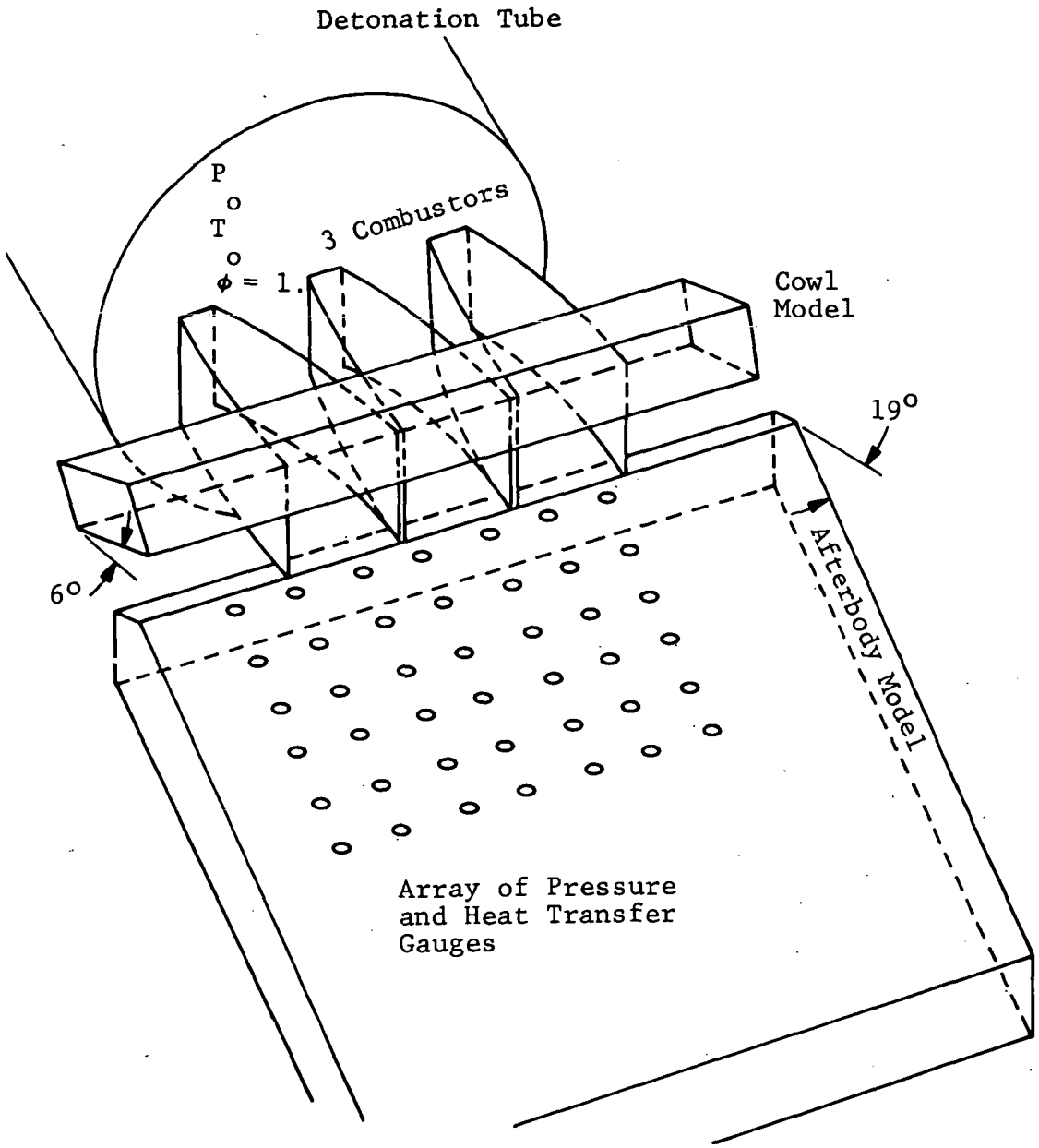

Fig. 11 Sketch of Detonation Tube and Model Installation for Segmented $\mathcal{A}_R$ = 3 Scramjet Combustor Exit Plane

TABLE 2

EQUILIBRIUM THERMODYNAMIC AND TRANSPORT PROPERTIES AT SCRJ COMBUSTOR EXIT PLANE WITH CORRESPONDING ISENTROPIC STAGNATION CONDITIONS

ϕ	0.6			1.0								
M_∞	4.0			6.0			8.0			10.		
$\alpha + \beta$ (deg)	4	8	12	4	8	12	4	8	12	4	8	12
COMBUSTOR EXIT PLANE CONDITIONS												
P_3 (atm)	1.0066	1.0367	1.0310	0.9090	1.2116	1.4289	0.5444	0.7880	1.0252	0.3995	0.5891	0.6817
T_3 (°K)	1745.	1724.	1734.	2334.	2332.	2317.	2305.	2314.	2360.	2348.	2339.	2256.
V_3 (m/sec)	1059.9	1089.7	1075.9	1606.1	1621.8	1650.0	2272.5	2275.0	2230.9	2854.9	2877.5	2954.9
M_3	1.266	1.309	1.289	1.657	1.672	1.704	2.362	2.357	2.290	2.949	2.972	3.095
A_3/A^*	1.0578	1.0775	1.0681	1.3755	1.3934	1.4319	3.1233	3.0833	2.8142	7.6528	7.8374	9.4151
Rey. No.$_3$ (m^{-1})	3.26×10^6	3.53×10^6	3.43×10^6	2.51×10^6	3.38×10^6	4.10×10^6	2.17×10^6	3.13×10^6	3.85×10^6	1.93×10^6	2.90×10^6	3.68×10^6
γ_3	1.2646	1.2661	1.2654	1.1818	1.1863	1.1904	1.1783	1.1825	1.1802	1.1675	1.1748	1.1887
m_3	26.178	26.179	26.179	24.415	24.440	24.463	24.401	24.423	24.401	24.318	24.371	24.464
μ_3 (μ poise)	598.	593.	595.	742.	742.	739.	735.	738.	748.	745.	743.	724.
$k_3\left(\frac{\mu\ cal}{cm\text{-}sec\text{-}°K}\right)$	320.	315.	317.	850.	801.	757.	883.	837.	878.	1053.	940.	757.
$c_{p_3}\left(\frac{cal}{gm\text{-}°K}\right)$	.3641	.3623	.3631	.6169	.5943	.5747	.6350	.6126	.6268	.7066	.6574	.5809
Pr_3	.6816	.6826	.6822	.5387	.5503	.5607	.5289	.5402	.5345	.4996	.5196	.5552
ISENTROPIC STAGNATION CONDITIONS												
P_o (atm)	2.528	2.761	2.672	3.900	5.341	6.637	8.20	11.73	13.40	19.63	30.20	45.07
T_o (°K)	2099.	2099.	2099.	2812.	2832.	2846.	3164.	3200.	3213.	3572.	3633.	3690.
H_o (cal/gm)	99.1	99.1	99.1	278.0	278.0	278.0	578.4	578.4	578.4	970.4	970.4	970.4
a_o (m/sec)	909.2	909.4	909.4	1062.1	1066.4	1069.3	1138.9	1145.0	1147.3	1235.8	1244.9	1253.1
γ_o	1.2390	1.2394	1.2393	1.1543	1.1571	1.1591	1.1470	1.1498	1.1508	1.1504	1.1534	1.1563
m_o	26.156	26.157	26.157	23.920	23.960	23.987	23.262	23.331	23.357	22.371	22.483	22.588

Note: 1 atm = 1.01325×10^5 N/m^2

required to achieve the desired Reynolds number, together with the other thermodynamic and transport properties at the model combustor exit plane.

Table 3 summarizes the results of these calculations for the $M_\infty = 8$ flight cases. The differences between the 1/8 scale model and prototype exit plane Mach numbers and other state properties may be seen by comparing Tables 2 and 3. Achieving a stagnation pressure between 60 and 110 atmospheres with backward-running detonations is no problem in our facility. We have repeatedly run different simulated propellants at pressures between 10 and 400 atmospheres. The driver pressure, P_4, requirements for these backward-running detonations are not at all severe — 10 to 20 atmospheres at the most.

To achieve stagnation pressures, P_5, of several hundred atmospheres with front-running detonations, higher driver pressures are required. For the Mach 8 flight cases using room temperature helium as the driver gas, the driver pressures will be between 200 and 300 atmospheres. We have routinely run forward-running detonations with P_4's between 300 and 400 atmospheres and have the capability to operate at double that level. Thus, simulating the $M_\infty = 8$ flight case with 1/8 scale models at full scale Reynolds number is well within the operating range of the Grumman Detonation Tube Simulator.

Ensuring that the edges of the exhaust expansion regions will be properly configured requires that the contact surfaces between external and internal gas in the detonation tube test lie outboard of the contact surfaces in the flight and wind tunnel cases. This is achieved by ensuring that the test chamber pressure in the detonation tube is well below the static pressure of the flight contact surface (i.e., the pressure at which internal and external flows can turn to the same flow direction). The domain of validity for the test is then determined analytically for each flight condition.

Experimental Verification of Simulation Technique

The next phase of this program will include proof-of-concept experiments to validate the proposed technique. During these experiments measurements of the wave speeds and stagnation pressure, P_5, will be made to insure that the desired stagnation conditions have been achieved. Calibration of the flow from the combustor exit will be accomplished by stagnation pressure and

TABLE 3

EQUILIBRIUM THERMODYNAMIC AND TRANSPORT PROPERTIES AT $\frac{1}{8}$-SCALE MODEL COMBUSTOR EXIT PLANE FOR SIMULATING FULL SCALE REYNOLDS NUMBER WITH CORRESPONDING DETONATION TUBE ISENTROPIC STAGNATION CONDITIONS, $M_\infty = 8.0$, $\phi = 1.0$

$\alpha + \beta$ (deg)	4	8	12
P_3 (atm)	4.2731	6.1788	8.0730
T_3 (°K)	2310.0	2316.0	2368.0
V_3 (m/sec)	2317.28	2316.93	2272.87
M_3	2.386	2.380	2.311
A_3/A^*	3.1233	3.0833	2.8142
Rey. No.$_3$ (m^{-1})	1.736×10^7	2.500×10^7	3.081×10^7
γ_3	1.2045	1.2077	1.2051
$\mathcal{M}_3$	24.524	24.536	24.522
μ_3 (μ poise)	738.0	739.0	752.0
k_3 $\left(\frac{\mu \text{ cal}}{\text{cm-sec-°K}}\right)$	642.0	622.0	650.0
c_{p_3} $\left(\frac{\text{cal}}{\text{gm-°K}}\right)$	0.5183	0.5073	0.5167
Pr_3	0.5953	0.6029	0.5979
DETONATION TUBE ISENTROPIC STAGNATION CONDITIONS			
P_5 (atm)	66.96	95.623	109.45
T_5 (°K)	3365.0	3397.0	3409.0
H_5 $\left(\frac{\text{cal}}{\text{gm}}\right)$	578.4	578.4	578.4
a_5 (m/sec)	1173.3	1178.7	1180.8
γ_5	1.1636	1.1665	1.1676
$\mathcal{M}_5$	23.651	23.712	23.735

Note: 1 atm = 1.01325×10^5 N/m^2

heat transfer surveys using instrumented rakes at several stations along the afterbody. A limited amount of spectroscopic/radiometric analysis for exhaust composition and temperature assessment will also be conducted.

Calculation procedures proven in previous plume simulation work (such as reported on in Ref. 9), will be used for comparison with the measured data. We have shown in the past that such comparisons give a valid indication of the fidelity of a given detonation tube simulation. In addition, IR measurements obtained in plumes simulated by the detonation technique have been shown to give remarkable agreement with other experimental techniques as well as with detailed theoretical calculations (Ref. 10). The methods used in such theoretical computations are presently limited to axisymmetric nozzles, so their application to the nonuniform three dimensional afterbody flow of this project will only be an intermediate step. Final and complete theoretical substantiation of our data in the flight situation must await the completion of theoretical methods now under development by other contractors.

TWO DIMENSIONAL AFTERBODY PRESSURE AND FORCE PREDICTIONS

The goal of this program is to provide a system of substitute gases for use in a wind tunnel model that will duplicate the distribution of forces produced by the scramjet engine exhaust over the vehicle afterbody. In this section we present calculations of pressure distributions for several different cases, and, in addition, show integrated axial and normal force values. All calculations in this section are for a flight Mach number of 8. The results are the basis of our conclusion that it is possible to select a substitute gas to fulfill the goal stated above.

We have performed two dimensional method of characteristics calculations for nine separate cases. For the full scale flight hydrogen/air combustion system, we did four calculations: equilibrium and exit plane frozen, each at inlet ramp angles $(\alpha + \beta)$ of $4°$ and $12°$. We have similarly calculated pressure distributions for an eighth scale detonation tube simulation, matching all conditions at the exit plane to that of full scale, but raising the pressure to duplicate Reynolds number. The eighth scale calculations were carried out for $\alpha + \beta$ of $4°$ and $12°$, but only for equilibrium chemistry. An exact nonequilibrium two dimensional kinetic calculation has not been carried out.

Three substitute gases were chosen using the methods described earlier to match the full scale case of $\alpha + \beta = 4°$ and equilibrium chemistry. The first consisted of 50 percent by volume Freon 13B1 and 50 percent argon, the second 40 percent Freon 12 and 60 percent argon, and the third 58 percent Freon 13B1 and 42 percent argon. Mach number and Reynolds number at the nozzle exit were matched for the substitute gas calculations. We also calculated a pressure distribution assuming $\gamma = 1.4$ air with the same exit Mach number as an illustration of the sensitivity of loads to large errors in gas characteristics.

In all cases the two dimensional method of characteristics computer program of Ref. 11 was employed. The thermodynamic variables for the combustion gases were generated by the computer program of Ref. 8, while those for the substitute gases were calculated as described in the appendix. The flow properties at the combustor exit were assumed uniform, parallel, and in equilibrium for all cases.

The geometrics of the afterbody nozzle surface and the cowl surface are described by the following equations:

Afterbody

$$\bar{Y} = 0.7187\ \bar{X}^2 + 1.0 \qquad 0 \leq \bar{X} \leq 0.25$$

$$\bar{Y} = 0.35935\ \bar{X} + 0.95508 \qquad 0.25 \leq \bar{X} \leq 18.54$$

Cowl

$$\bar{Y} = 0 \qquad 0 \leq \bar{X} \leq 1.11$$

$$\bar{Y} = -0.4204\ \bar{X}^2 + 0.933\ \bar{X} - 0.518 \qquad 1.11 \leq \bar{X} \leq 1.235$$

$$\bar{Y} = -0.1051\ \bar{X} + 0.1232 \qquad 1.235 \leq \bar{X} \leq 3.12$$

where $\bar{Y} = Y/Y_3$, $\bar{X} = X/Y_3$, and Y_3 is the height of the nozzle exit.

A sketch of this geometry showing the origin of the coordinates is shown in Fig. 12. Also shown in this figure is the characteristic diagram calculated for the full scale engine, for $M_\infty = 8$, $\alpha + \beta = 12°$, and assuming fully equilibrium flow. The flow fields for all other cases mentioned above with the exception of the air case differed from the one shown only in small detail. Regions of uniform flow are labeled "U." At the cowl lip there is a Prandtl-Meyer expansion to match the local external pressure. In all of the cases considered except the $\gamma = 1.4$ case the first characteristic line from the lip intersected the upper surface at $\bar{X} \approx 15.5$. The characteristic line that intersects the downstream end of the upper surface corresponds to an expansion of about 3° (through a pressure ratio of 1.15). It has been shown that the turning pressure ratio at the cowl lip is close to 2 for the prototype flight case. This point is very important, as it indicates that at least for two dimensional testing the internal flow is all that need be simulated to ensure that the afterbody ramp pressures are valid. Mixing effects are not likely to destroy this independence of the external flow as long as the combustor exit is everywhere underexpanded, but three dimensional effects at the ends of the combustor will require more complete simulation for regions near and outside the diverging lateral contact surfaces.

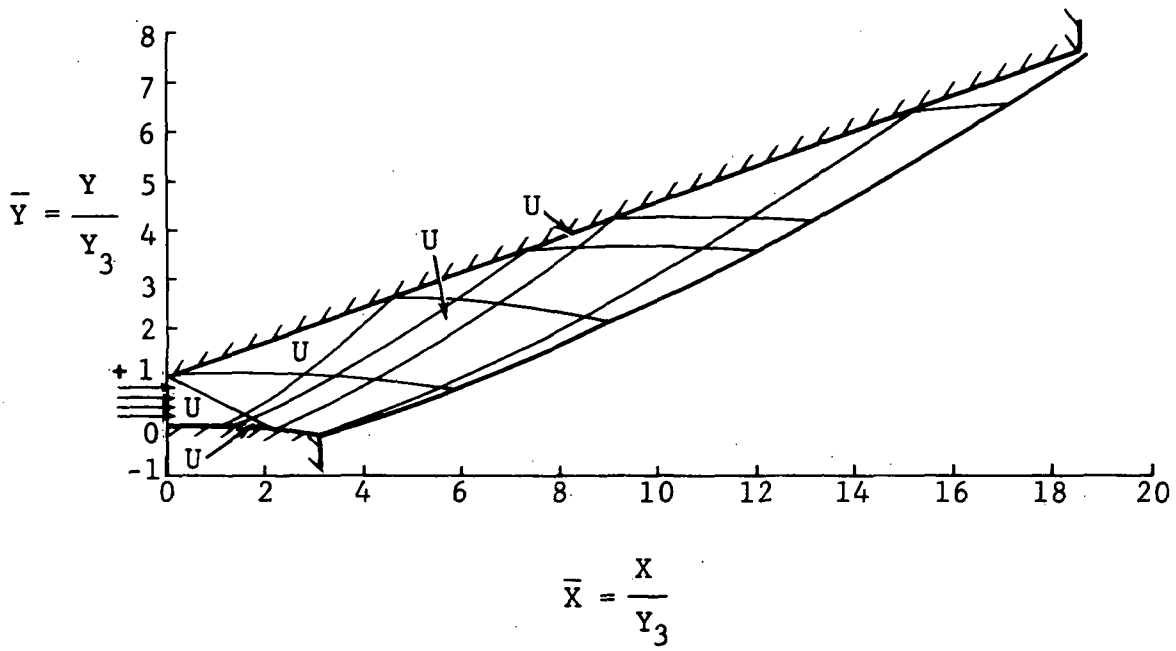

Fig. 12 Nozzle Afterbody Geometry and Characteristic Diagram for Full-Scale Engine at $M_\infty = 8, \alpha+\beta = 12°$

In Fig. 13 we have plotted the pressure distributions, nondimensionalized by the combustor exit plane pressure for each case, for the combustion gases at exit conditions corresponding to $\alpha + \beta = 4°$. In Fig. 14, we show pressure distributions for $\alpha + \beta = 12°$. It can be seen that the pressures calculated assuming fully equilibrium flow are slightly higher than those calculated using frozen chemistry. Also the excellent agreement with the case calculated for the detonation tube simulation is evident. In Fig. 15 we have compared the calculated pressures for the eighth scale detonation tube simulation with those calculated for the three substitute gas mixtures for an $\alpha + \beta$ of $4°$. For comparison we have shown the pressure distribution that would be obtained by expanding air at a constant γ of 1.4, assuming the exit Mach number matches that of the actual engine.

We have integrated the pressure distributions shown in Figs. 13 through 15 to obtain relative values for the forces in the normal and axial direction. We normalize the two dimensional forces by P_3A, where A is the (unit) width times L, the afterbody length. We have not calculated any pitching moment changes, because the shifts in center of pressure are extremely small. Figure 16 is a bar graph comparing all of the forces calculated for the case of $\alpha + \beta = 4°$, and Fig. 17 is a comparison of those for the $\alpha + \beta = 12°$ case. The differences in normal force between frozen and equilibrium flow appear to be more significant than a quick look at the pressure distributions would indicate. This apparent disparity exists because the net normal forces are only 20 to 30 percent of the individual (cowl or afterbody) normal forces, and the percentage change in pressure level introduced by chemical reaction is much greater on the afterbody than it is on the cowl lip. The detonation tube simulation falls between the two cases. The axial forces are all within a few percent of one another with the exception of the constant $\gamma = 1.4$ air case. Of the three substitute gas mixtures chosen for this comparison, 50 percent Freon 13B1 and 50 percent argon can be seen to give forces very close to the equilibrium full scale engine, and the detonation tube simulation lies between the frozen and equilibrium values. Once the true chemical state of the real engine exhaust flow field is known, there should be no trouble selecting a substitute gas to match the pressure distribution to any required system fidelity.

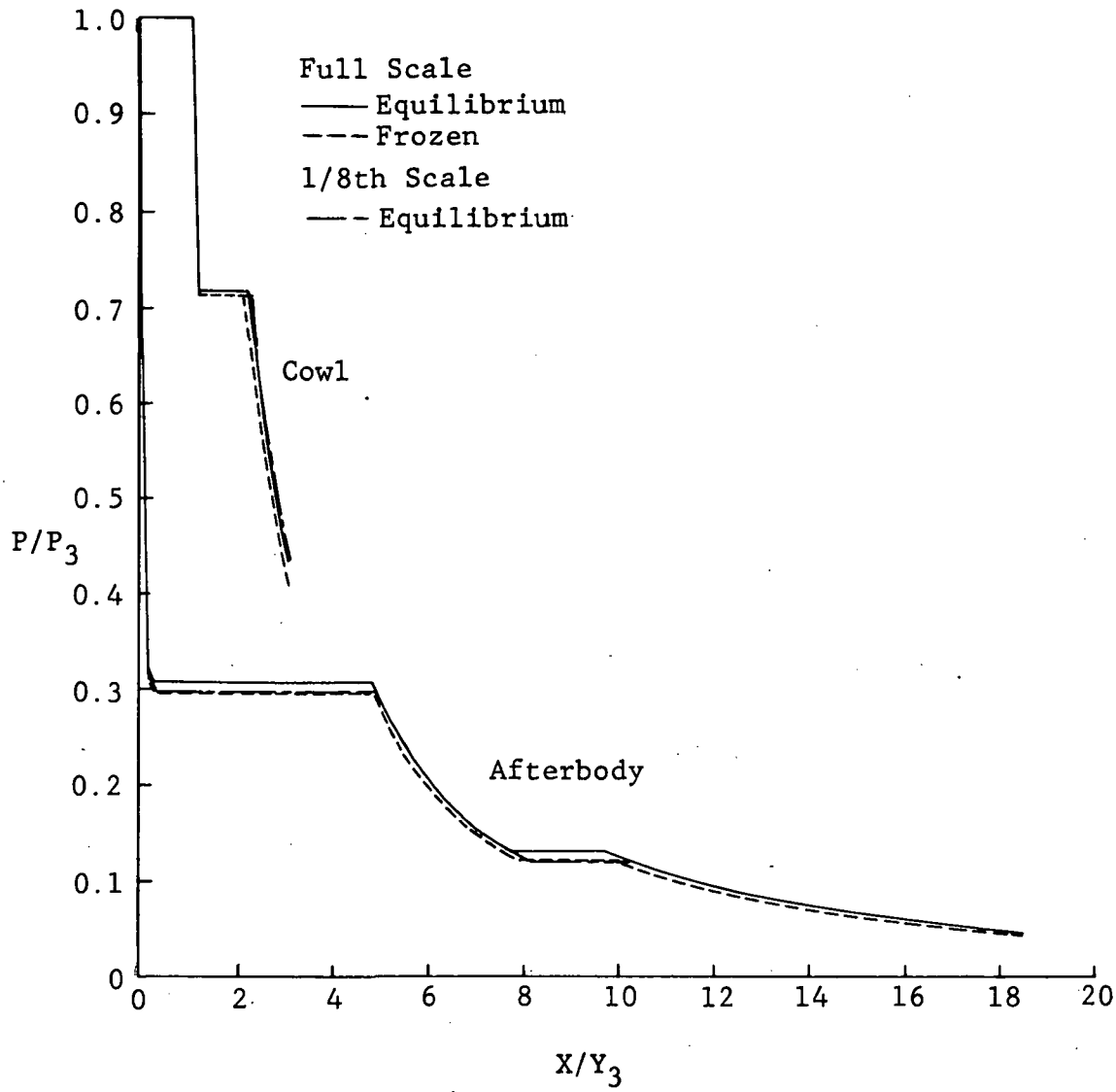

Fig. 13 Flight Afterbody Pressure Distributions - Combustion Gases, $M_\infty = 8, \alpha + \beta = 4°$

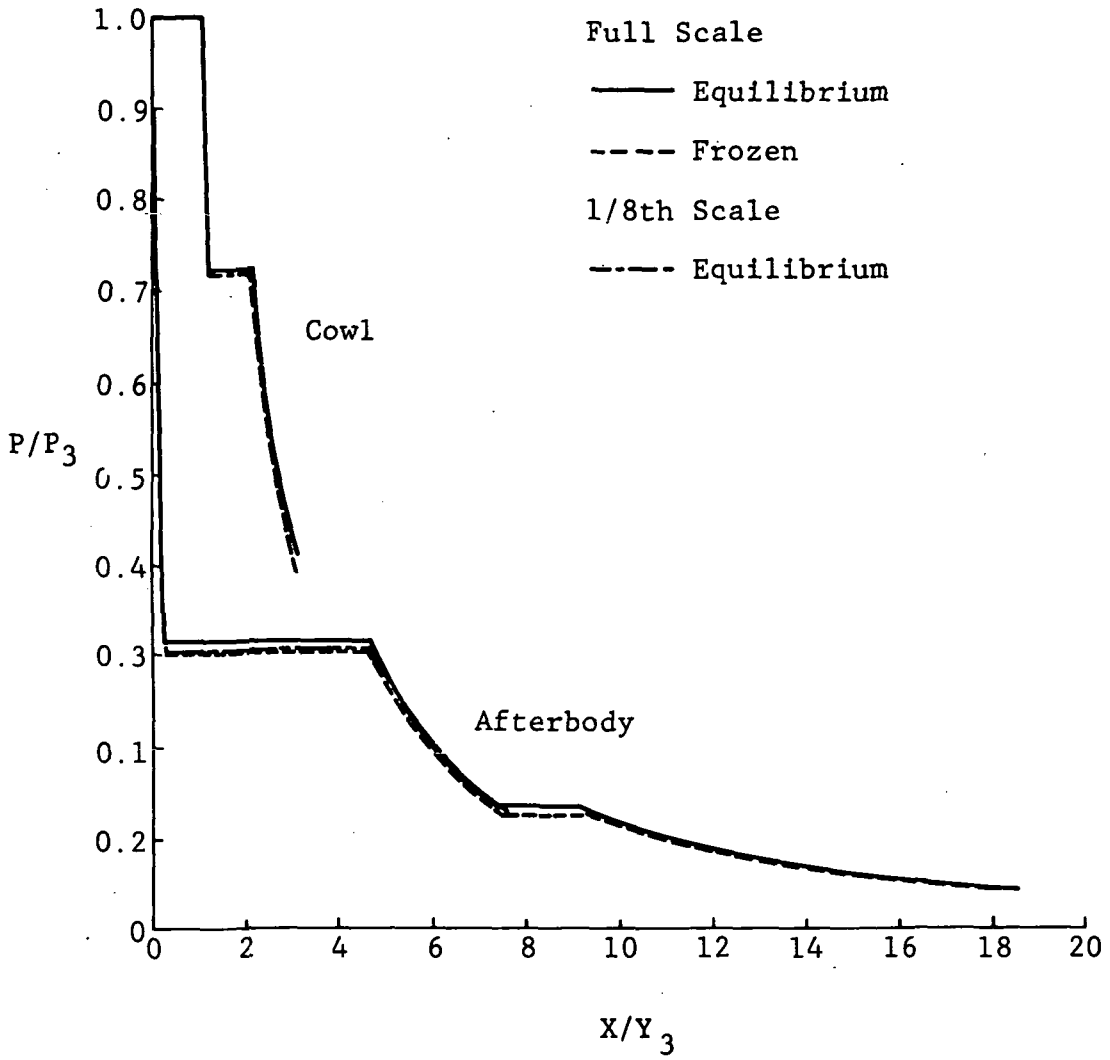

Fig. 14 Flight Afterbody Pressure Distributions - Combustion Gases, $M_\infty = 8, \alpha + \beta = 12^o$

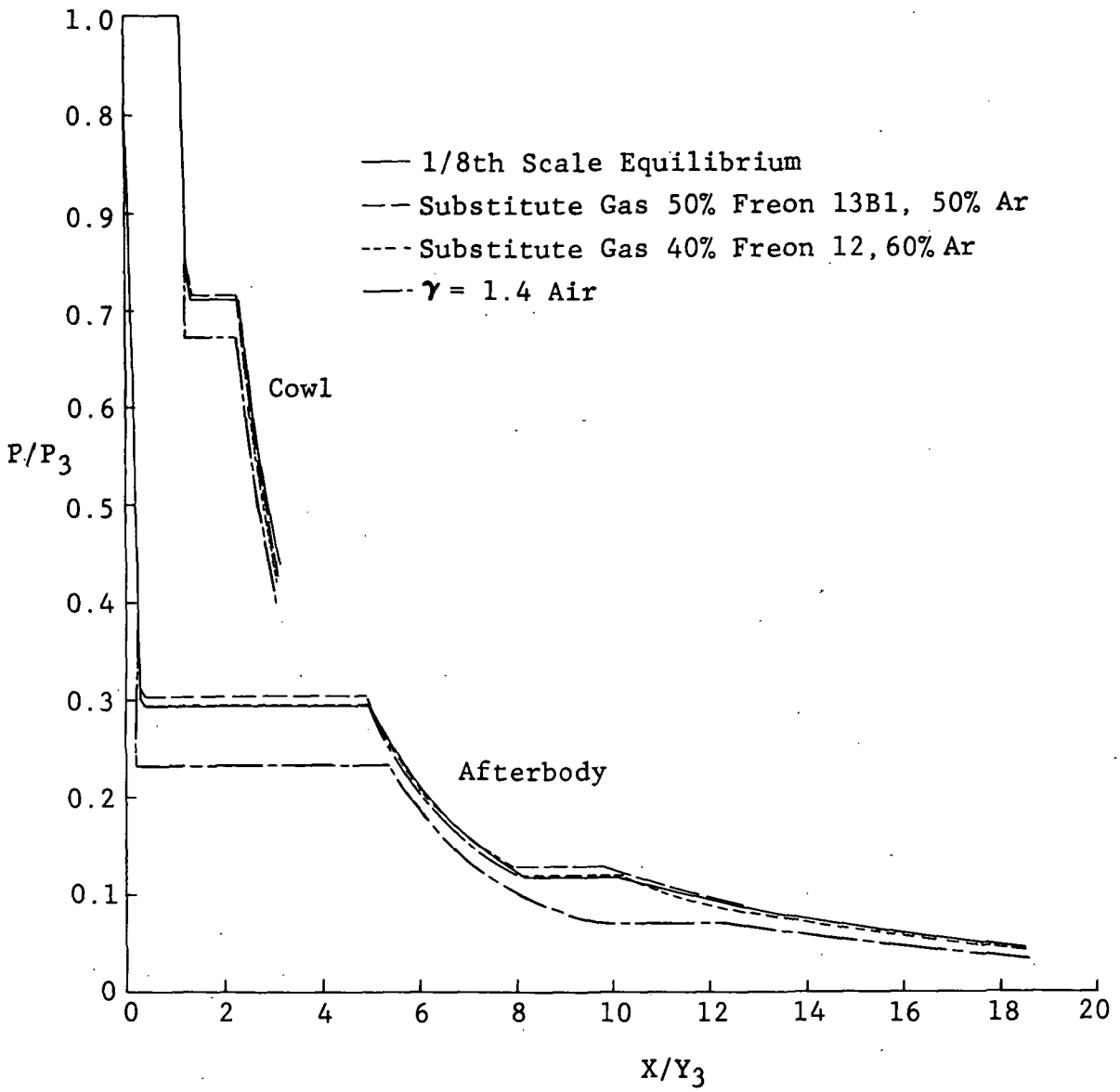

Fig. 15 Simulated Afterbody Pressure Distributions, $M_\infty = 8, \alpha + \beta = 4°$

Relative Normal Forces

$$\frac{Fy}{P_3 A} = \frac{1}{L}\int \frac{P}{P_3}\, d(x)$$

Prototype - Equilibrium	0.0339	
Prototype - Frozen	0.0279	
Model - 1/8th Scale Det. Tube	0.0301	
Model - Sub. Gas	0.0339	50% Freon 13 B1, 50% Ar
Model - Sub. Gas	0.0292	40% Freon 12, 60% Ar
Model - Sub. Gas	0.0344	58% Freon 13 B1 + 42% Ar
0.00351	Const. γ (=1.4)	

Relative Axial Forces

$$\frac{Fx}{P_3 A} = \frac{1}{L}\int \frac{P}{P_3}\, d(y)$$

Prototype - Equilibrium	0.0648
Prototype - Frozen	0.0620
Model - 1/8th Scale Detonation Tube - Equilibrium	0.0634
Model - Sub. Gas - 50% Freon 13B1, 50% Ar	0.0646
Model - Sub. Gas - 40% Freon 12, 60% Ar	0.0627
Model - Sub. Gas - 58% Freon 13 B1 + 42% Ar	0.0647
Const.γ (=1.4)	0.0520

Fig. 16 Normal and Axial Forces for 2D Expansions
$M\infty = 8, \alpha + \beta = 4^{o}$

Relative Normal Forces

$$\frac{Fy}{P_3 A} = \frac{1}{L}\int \frac{P}{P_3}\, d(x)$$

Prototype - Equilibrium	0.0351
Prototype - Frozen	0.0296
Model - 1/8th Scale Det. Tube	0.0316

Relative Axial Forces

$$\frac{Fx}{P_3 A} = \frac{1}{L}\int \frac{P}{P_3}\, d(y)$$

Prototype - Equilibrium	0.0647
Prototype - Frozen	0.0622
Model - 1/8th Scale Detonation Tube - Equilibrium	0.0634

Fig. 17 Normal and Axial Forces for 2D Expansions
$M_\infty = 8$, $\alpha + \beta = 12^\circ$

CONCLUSIONS

There are several substitute gas blends that should give excellent representations of the pressure, force, and moment distributions for scramjet exhaust flows over vehicle afterbodies. These binary gas mixtures can be used in wind tunnels and in a shock tunnel, and they show excellent promise for representing the viscous behavior of the SCRJ flow as well as its inviscid characteristics. Different blends can be designed to compensate for small differences in the expected chemical reaction rates of the flight engine or for changes in flight conditions.

The detonation tube system provides the best available laboratory simulation of the chemical, dynamic, and thermodynamic behavior of the flight SCRJ exhaust. This enables the detonation tube to be used as a standard of comparison against which substitute gas representations of the flight pressure distribution can be evaluated.

Analysis shows that relatively small changes in flow thermochemistry and resultant pressure distributions can produce significant changes in vehicle loading, especially in afterbody normal force. This means that the efforts to overcome the difficulties of creating and employing accurate methods of matching pressure distributions are, in fact, necessary, and that even relatively minor three dimensional flow details will need careful study in later stages of development.

Proof-of-concept tests are required to show that the analytically predicted matching of the SCRJ exhaust can be realized in practice. These tests will also indicate the degree to which the detonation tube system can be used to investigate the effects of three dimensional flow details such as the dividers between segments of the combustor.

There is a need to develop a better understanding of the similitude requirements for the viscous mixing layer between internal and external flow. If complete fidelity to all possible similitude requirements is enforced, the external flow will have to be of very low temperature or very high molecular weight, e.g., chilled Freon gas. It is likely that these constraints could be relaxed significantly to allow a much simpler test system, but only after experiments on the hypersonic mixing layer have shown

this to be permissible. We suggest that another set of experiments be planned and conducted while the detonation tube proof-of-concept is under way, so that ultimate wind tunnel testing will be as simple as possible without loss of validity.

REFERENCES

1. Hopkins, H., Konopka, W., Leng, J., and Oman, R., "Simulation Experiments Using Hydrogen/Oxygen Gas Mixtures in a High-Pressure Detonation Tube," Final Report, Contract No. NAS 9-12447, Grumman Research Department Report RE-456, May 1973; also published as NASA Report MSC-05836.

2. Goldstein, S. (Ed.), Modern Developments in Fluid Dynamics, Vol. 1, Oxford: Clarendon Press, 1938.

3. Griffith, W., "Vibrational Relaxation Times in Gases," J. Appl. Phys., Vol. 21, No. 12, pp. 1319-1325, December 1950.

4. Ferri, A., "Mixing Controlled Supersonic Combustion," in Annual Review of Fluid Mechanics, Vol. 5, Annual Reviews, Inc., Palo Alto, California, p. 319, 1973.

5. Leng, J. and Oman, R., "On the Simulation of Hypersonic Scramjet Engine Plumes in a Detonation Tube Facility," Grumman Research Department Note RN-339, December 1972.

6. Jones, R. and Hunt, J., "Use of Tetrafluoromethane to Simulate Real-Gas Effects on the Hypersonic Aerodynamics of Blunt Vehicles," NASA TR-R-312, June 1969.

7. Huber, P. W., "Use of Freon-12 as a Fluid for Aerodynamic Testing," NACA TN-1024, April 1946.

8. Svehla, R. and McBride, B., "FORTRAN IV Computer Program for Calculation of Thermodynamic and Transport Properties of Complex Chemical Systems," NASA TN-D-7056, January 1973.

9. Leng, J., Oman, R., and Hopkins, H., "A Detonation Tube Technique for Simulating Rocket Plumes in a Space Environment," J. Spacecraft and Rockets, Vol. 5, No. 10, pp. 1148-1154, October 1968.

10. Slack, M. W., "Measurements of Infrared and Vacuum Ultraviolet Radiation from Simulated Rocket Exhaust Plumes (U)," Final Contract Report No. S-046-277, Grumman Research Department Report RE-465, 15 December 1973 (SECRET).

11. Ratliff, A., Smith, S., and Penny, M., "Rocket Exhaust Plume Computer Program Improvement, Volume I - Final Report, Summary Volume, Method-of-Characteristics Nozzle and Plume Programs," Lockheed Missiles and Space Company Report LMSC/HREC D162220-1, January 1972.

APPENDIX

CALCULATION METHODS FOR SUBSTITUTE GAS MIXTURES

A. Thermodynamic Properties

The usual thermodynamic properties of homogeneous mixtures of two or more gases are computed from the component gas properties by use of the relationships:

a) $\gamma_m = \dfrac{\Sigma X_i c_{p_i}}{\Sigma X_i (c_{p_i} - R)}$ - ratio of specific heats

b) $\mathcal{M}_m = \Sigma X_i \mathcal{M}_i$ - molecular weight

c) $H_m = \Sigma X_i H_i$ - enthalpy

d) $S_m = \Sigma X_i S_i$ - entropy

e) $P_m/\rho_m = RT_m/\mathcal{M}_m$ - gas law

where X_i is the mole (volume) fraction of each component of the mixture.

B. Transport Properties

The transport properties, viscosity, thermal conductivity, and mutual diffusivity of binary and ternary mixtures are determined by mixture estimation formulas.

For viscosity, the Wilke method (Ref. A-1) has been employed because it yields results rapidly and has been verified by many experimental measurements and found to give comparable accuracy to the rigorous kinetic-theory relations (Ref. A-2). The Wilke relation for a binary mixture viscosity is:

$$\mu_m = \frac{\mu_1}{\left[1 + \dfrac{X_2}{X_1}\varphi_{12}\right]} + \frac{\mu_2}{\left[1 + \dfrac{X_1}{X_2}\varphi_{21}\right]}$$

where

μ = viscosity, (gm/cm - sec) x 10^{-6} (micropoise)

X_1, X_2 = mole fraction of gas component 1 and 2, respectively

$$\varphi_{12} = \left[1 + \left(\frac{\mu_1}{\mu_2}\right)^{\frac{1}{2}} \left(\frac{m_2}{m_1}\right)^{\frac{1}{4}}\right]^2 \left[8\left(1 + \frac{m_1}{m_2}\right)\right]^{-\frac{1}{2}}$$

$$\varphi_{21} = \varphi_{12}\left(\frac{\mu_2}{\mu_1}\right)\left(\frac{m_1}{m_2}\right)$$

m = molecular weight of gas component.

Average deviations of computed values from data for many binary mixtures have been reported as typically one percent for the Wilke equation; this is considered adequate for our purposes.

The viscosity estimation equation for a ternary mixture by Wilke's method takes the general form:

$$\mu_m = \sum_{i=1}^{3} \mu_i \left[1 + \sum_{\substack{j=1 \\ j \neq i}}^{3} \varphi_{ij}(X_j/X_i)\right]^{-1}$$

where φ_{12} and φ_{21} have been previously defined, and

$$\varphi_{13} = \left[1 + \left(\frac{\mu_1}{\mu_3}\right)^{\frac{1}{2}} \left(\frac{m_3}{m_1}\right)^{\frac{1}{4}}\right]^2 \left[8\left(1 + \frac{m_1}{m_3}\right)\right]^{-\frac{1}{2}}$$

$$\varphi_{31} = \varphi_{13}\left(\frac{\mu_3}{\mu_1}\right)\left(\frac{m_1}{m_3}\right)$$

$$\varphi_{23} = \left[1 + \left(\frac{\mu_2}{\mu_3}\right)^{\frac{1}{2}} \left(\frac{m_3}{m_2}\right)^{\frac{1}{4}}\right]^2 \left[8\left(1 + \frac{m_2}{m_3}\right)\right]^{-\frac{1}{2}}$$

$$\varphi_{32} = \varphi_{23}\left(\frac{\mu_3}{\mu_2}\right)\left(\frac{m_2}{m_3}\right)$$

We have selected the Mason-Saxena (Ref. A-3) estimation method for determining thermal conductivity, k_m, of binary mixtures. This method is a simplified version of the classic Wassiljewa formulation, has the similar convenient form of the Wilke equation for mixture viscosity, and yields, typically, errors of less than 2 percent from actual data. The Mason-Saxena equation for binary mixtures is:

$$k_m = \frac{k_1}{1 + \frac{X_2}{X_1}\left[\frac{1.065\left(1 + \left(\frac{\mu_1}{\mu_2}\right)^{\frac{1}{2}}\left(\frac{m_2}{m_1}\right)^{\frac{1}{4}}\right)^2}{\left[8\left(1 + \frac{m_1}{m_2}\right)\right]^{\frac{1}{2}}}\right]} + \frac{k_2}{1 + \frac{X_1}{X_2}\left[\frac{1.065\left(1 + \left(\frac{\mu_2}{\mu_1}\right)^{\frac{1}{2}}\left(\frac{m_1}{m_2}\right)^{\frac{1}{4}}\right)^2}{\left[8\left(1 + \frac{m_2}{m_1}\right)\right]^{\frac{1}{2}}}\right]}$$

with units of cal/cm - sec - °K where the subscripts 1, 2, m refer to the two gas components and the binary mixture properties, respectively.

Another transport property needed for two similarity parameters is the diffusion coefficient for a binary gas system. This

coefficient is independent of component gas concentration and quantifies the mutual diffusion of the gas mixture components for an isothermal process.

The binary diffusion coefficient, D_{12}, has been computed with the theoretical equation derived from modern nonuniform gas theory, using a Lennard-Jones model to characterize the molecules, where:

$$D_{12} = 0.001858\ T^{3/2}\ \frac{\left[(m_1 + m_2)/(m_1 m_2)\right]^{\frac{1}{2}}}{P\sigma_{12}^2 \Omega_D}\ ,\quad cm^2/sec$$

where P is pressure in atmospheres and T is temperature in °K. The diffusion collision integral, Ω_D, is tabulated (Ref. A-2) as a function of the normalized temperature, $T/(\epsilon/k)$, where the molecular attraction law constant, ϵ/k, for the mixture is obtained by use of the combining rule:

$$(\epsilon/k)_{12} = \left[(\epsilon/k)_1\ (\epsilon/k)_2\right]^{\frac{1}{2}}$$

Similarly, the molecular collision diameter constant, σ_{12}, for the gas mixture is determinable from the rule:

$$\sigma_{12} = \tfrac{1}{2}(\sigma_1 + \sigma_2)$$

where the component σ's as well as (ϵ/k)'s were obtained principally from Svehla's (Ref. A-4) listing.

As a result of the computational investigation we have performed, the effect of the monomolecular gas additive in binary mixtures with Freon compounds can be characterized for several similarity parameters as follows:

- For sufficiently high initial temperature to avoid phase change during an expansion process, increasing the additive increases the value of γ.
- For a given initial temperature, pressure, and model size, increasing the additive fraction decreases the Reynolds number. As a result the model size for matching the full scale Reynolds number of the SCRJ increases

as additive is increased at the same pressure. Fortunately, these blends are all much higher in molecular weight than air, so they produce higher Re at small scale, and matching is not difficult.

- For a given initial temperature, the Mach number is matched at increasingly greater flow velocities in the model as the additive is increased. However, the model exhaust velocity is much lower than in the full scale apparatus.

- For a given initial temperature, the Prandtl number decreases with increase in additive fraction. The substitute gas mixtures have a similar but slightly greater magnitude of Prandtl number compared to the SCRJ combustion products.

- For a given initial temperature, the Schmidt number increases with increase in additive fraction. Both the substitute gases and SCRJ combustion products have similar magnitude of Schmidt numbers with the latter slightly greater.

- The transport properties of viscosity and thermal conductivity increase with increase in additive fraction. The viscosity of a substitute gas in its proper operating range is generally about one third that of the SCRJ exhaust, and the thermal conductivity is more than an order of magnitude smaller than that of the hot SCRJ gases.

- The mutual diffusivity of binary mixtures is greater than the single Freon-type component but is independent of mixture composition. The hot SCRJ exhaust gases have about two and one half orders of magnitude greater diffusivity than the relatively cool binary mixtures considered as substitute gases.

C. One Dimensional Gas Dynamics

The one dimensional gas dynamic properties of a substitute gas mixture flow have been determined with a minicomputer program, assuming an isentropic process and a thermally perfect gas. To justify these assumptions for the calorically imperfect (i.e., $\gamma \neq$ constant) binary gas mixtures, an over-all flow process has

been calculated on the basis of a series of small sequential step changes in temperature. An average γ for the incremental change is determined, and used in calculating the new flow properties at the end of the step change, using the equations:

$$P_2/P_1 = (T_2/T_1)^{\bar{\gamma}/\bar{\gamma}-1}$$

$$\rho_2/\rho_1 = (T_2/T_1)^{\frac{1}{\bar{\gamma}-1}}$$

where 1 and 2 denote the beginning and end conditions, respectively, of the chosen small step interval in temperature:

$$T_2/T_1 = \tau \quad ,$$

and

$$\bar{\gamma} \quad = \frac{\gamma_1 + \gamma_2}{2} \quad .$$

It is further assumed that across the small step, $T_{o_1} \simeq T_{o_2}$, and the new Mach number at the end of the step change is found by:

$$M_2^2 = \frac{2}{\bar{\gamma}-1}\left[\frac{1}{\tau} - 1\right] + \frac{M_1^2}{\tau} \quad .$$

The calculation starts with inputs of initial values of M, γ, T, and p based on matching of substitute gas mixtures to SCRJ exhaust gas properties. Generally, the Mach number is taken as the value at the combustor exit station, assuming homogeneous flow profiles. Initial values of γ, T, and P are taken to match SCRJ combustor exit γ_3 and Re, although the value of T can be selected for convenient test facility operation; the initial value of P can be taken as one and corrected for exact Re matching at a later time. Similarly, the value of initial γ_m can be taken as a value greater than the SCRJ γ_3 so as to produce an over-all substitute gas expansion process that better approximates the SCRJ process.

The γ_m variation with temperature for a particular binary mixture is precalculated using Eq. (a) of Section A of this appendix, and the JANAF table data of c_p for different temperatures

of each mixture component. These discrete calculated values of γ_m are curve fitted by a third order polynomial in T, stored in the minicomputer, and retrieved in the gas dynamic program to yield values of γ_m for each new temperature in the stepwise calculations through the flow channel.

Additional inputs needed to commence the computation are the individual values of τ to be used and the total number of prescribed repetitive steps. For directing the calculation to increasing values of M beyond the initial value, τ is taken as slightly less than unity (e.g., 0.97). For decreasing values of M toward the stagnation point (M = 0), a value of τ slightly greater than 1 (e.g., 1.01) is selected. As the calculation approaches M = 0, an ongoing test for the next step being projected beyond M = 0 (i.e., to a virtual negative M) stops the calculation at the current step. If a finer grid size is desired to obtain nearly stagnation state conditions, the computation can be restarted at any small subsonic Mach number with a value for τ closer to 1 than previously used. It has been found that a final $\tau = 1.0001$ usually is sufficient to obtain stagnation state conditions to five figure accuracy in temperature.

Table A-1 presents representative results of the one dimensional gas dynamic calculations for three good substitute gas binary mixtures. These results have been used in the two dimensional method of characteristics computations described elsewhere in this report in the Two Dimensional Afterbody Pressure and Force Prediction section.

TABLE A-1

REPRESENTATIVE ONE DIMENSIONAL GAS DYNAMIC PROPERTIES FOR THREE SUBSTITUTE GAS MIXTURES

Substitute Gas Mixture	M Mach No.	$\mathcal{M}$ Molecular Wt.	γ	T (°K)	P (N/m^2)	P (atm)
50% Freon 13B1+ 50% Argon	1.3088	94.42	1.1795	539.123	2.558×10^5	2.5247
	1.7205		1.1853	488.066	1.286×10^5	1.2693
	2.0287		1.1911	446.26	7.126×10^4	0.7033
	2.36		1.1994	400.00	3.607×10^4	0.356
	2.9691		1.2181	324.00	1.065×10^4	0.1051
	3.5295		1.2407	262.44	3.486×10^3	0.0344
	4.0662		1.2667	212.576	1.274×10^3	0.01257
	4.5885		1.2970	172.1865	5.168×10^2	0.0051
	5.1113		1.3304	139.471	2.330×10^2	0.0023
40% Freon 12 + 60% Argon	1.4519	72.324	1.2054	533.756	1.891×10^5	1.866
	1.7051		1.2092	497.875	1.233×10^5	1.217
	2.0224		1.2153	450.725	6.829×10^4	0.674
	2.3314		1.2232	404.0	3.678×10^4	0.363
	2.6537		1.2328	360.0	1.978×10^4	0.1952
	3.2078		1.2531	291.6	6.758×10^3	0.0667
	3.7313		1.2788	236.2	2.530×10^3	0.02497
	4.2441		1.3079	191.318	1.044×10^3	0.0103
	4.7479		1.3423	154.97	4.762×10^2	0.0047
	5.0046		1.3600	139.47	3.344×10^2	0.0033
58% Freon 13B1+ 42% Argon	1.5466	103.15	1.1786	401.98	1.284×10^6	12.67
	2.299		1.1951	329.45	2.634×10^5	2.60
	2.365		1.197	322.96	2.270×10^5	2.24
	2.655		1.2056	295.30	1.196×10^5	1.18
	2.9025		1.2142	272.70	6.961×10^4	0.687
	3.173		1.2244	249.35	3.941×10^4	0.389
	3.4099		1.2338	230.27	2.452×10^4	0.242
	3.821		1.2508	200.33	1.150×10^4	0.1135
	3.9977		1.2594	188.72	8.542×10^3	0.0843
	4.06		1.260	185.0	7.751×10^3	0.0765

REFERENCES

A-1 Wilke, C., "A Viscosity Equation for Gas Mixtures," J. Chem. Phys., Vol. 18, p. 517, 1950.

A-2 Hirschfelder, J., Curtiss, C., and Bird, R., Molecular Theory of Gases and Liquids, J. Wiley and Sons, New York, 1954.

A-3 Mason, E. and Saxena, S., "Approximate Formula for the Thermal Conductivity of Gas Mixtures," Phys. Fluids, Vol. 1, p. 361, 1958.

A-4 Svehla, R. A., "Estimated Viscosities and Thermal Conductivities of Gases at High Temperatures," NASA TR R-132, 1962.

NATIONAL AERONAUTICS AND SPACE ADMINISTRATION
WASHINGTON, D.C. 20546

OFFICIAL BUSINESS
PENALTY FOR PRIVATE USE $300

SPECIAL FOURTH-CLASS RATE BOOK

POSTAGE AND FEES PAID
NATIONAL AERONAUTICS AND SPACE ADMINISTRATION
451

U.S.MAIL

POSTMASTER: If Undeliverable (Section 158 Postal Manual) Do Not Return

"The aeronautical and space activities of the United States shall be conducted so as to contribute . . . to the expansion of human knowledge of phenomena in the atmosphere and space. The Administration shall provide for the widest practicable and appropriate dissemination of information concerning its activities and the results thereof."

—NATIONAL AERONAUTICS AND SPACE ACT OF 1958

NASA SCIENTIFIC AND TECHNICAL PUBLICATIONS

TECHNICAL REPORTS: Scientific and technical information considered important, complete, and a lasting contribution to existing knowledge.

TECHNICAL NOTES: Information less broad in scope but nevertheless of importance as a contribution to existing knowledge.

TECHNICAL MEMORANDUMS: Information receiving limited distribution because of preliminary data, security classification, or other reasons. Also includes conference proceedings with either limited or unlimited distribution.

CONTRACTOR REPORTS: Scientific and technical information generated under a NASA contract or grant and considered an important contribution to existing knowledge.

TECHNICAL TRANSLATIONS: Information published in a foreign language considered to merit NASA distribution in English.

SPECIAL PUBLICATIONS: Information derived from or of value to NASA activities. Publications include final reports of major projects, monographs, data compilations, handbooks, sourcebooks, and special bibliographies.

TECHNOLOGY UTILIZATION PUBLICATIONS: Information on technology used by NASA that may be of particular interest in commercial and other non-aerospace applications. Publications include Tech Briefs, Technology Utilization Reports and Technology Surveys.

Details on the availability of these publications may be obtained from:

SCIENTIFIC AND TECHNICAL INFORMATION OFFICE

NATIONAL AERONAUTICS AND SPACE ADMINISTRATION

Washington, D.C. 20546